Sound Assembly of Dorsal Root Ganglion Multicellular System

E. Marani[1], J. Ma[1], M. Alini[1], T. Serra[1]

[1]*AO Research Institute, AO Foundation, Davos, CH*

INTRODUCTION: The culture of dorsal root ganglion (DRG) cells is a useful model in the study of pain-associated mechanism. Typical monolayer culture loses the multicellular structure which can be important for interneuronal communications. We use the sound induced morphogenesis method (SIM) to aggregate DRG cells into a multicellular system *in vitro* [1]. The influence of aggregation scale on hypoxic and necrosis core was investigated. Effect of the multicellular structure on calcium signal synchronization was evaluated.

METHODS: DRG cell line ND7/23 were aggregated into different scales of multicellular structure by tuning cell seeding densities (0.1 M cells/ml, 0.2 M cells/ml, 0.4 M cells/ml, 0.6 M cells/ml, 0.8 M cells/ml) (Fig. 1) in a 0.5 mg/mL collagen gel. Immunofluorescence of Hypoxia Inducible Factor 1 Subunit Alpha (HIF-1α) was performed to evaluate hypoxic response of cells and Ethidium-homodimer-1 staining was used to detect cell necrosis. Cells cultured in collagen gel without SIM served as control. The neuronal discharge was captured using calcium imaging (Fluo-4) [2]. In each culture, 5000 pairs of neurons were randomly sampled to investigate the neuronal synchronization which was calculated as numbers of simultaneous discharges of these 2 neurons divided by their total number of discharges. The influence of SIM on neuronal synchronization was evaluated.

RESULTS: HIF-1α expression in the middle of SIM-aggregated multicellular structure was down-regulated when the seeding density was lower than 0.4 M cells/ml (Fig. 2ab). Necrosis core could be avoided at the cell seeding density lower than 0.8 M cells/ml (Fig. 2c). Higher neuronal synchronization was found in SIM group at cell seeding density of 0.2 M cells/ml comparing to non-SIM control (Fig. 3).

DISCUSSION & CONCLUSIONS: DRG cells can be aggregated into multicellular structure with a scale that can be controlled by cell seeding density. Even without vascularization, a well-controlled scale of the *in vitro* cultured multicellular system can avoid hypoxic core and necrosis in cell aggregates. The multicellular system allows a better interneuronal communication to form the synchronized neuronal discharge which has been formerly observed *in vivo* [3]. Thus, the multicellular culture system not only recapitulate the complexity of *in vivo* structure but is also important for development *in vivo* function.

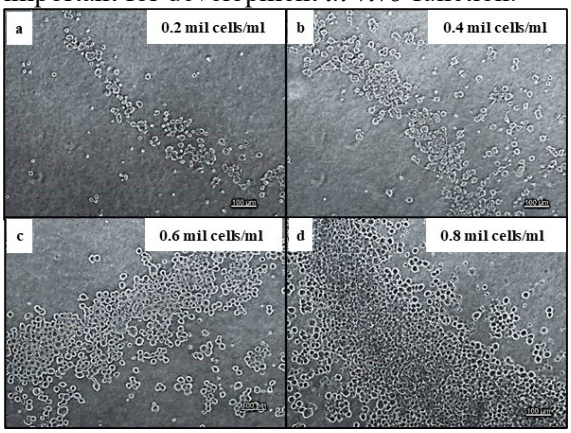

Fig. 1: Multicellular scale tuned by cellular concentration (a to d). Scale bars: 100 µm.

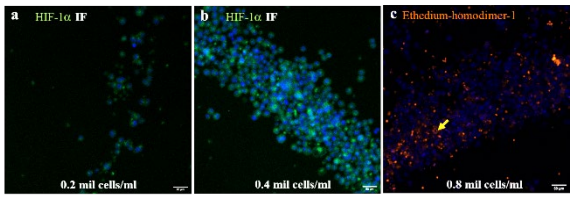

Fig. 2: Hypoxia-associated HIF-1α expression (b) and necrosis (yellow arrow) (c) can be avoided by tuning the multicellular scale (a). Scale bars: 50 µm.

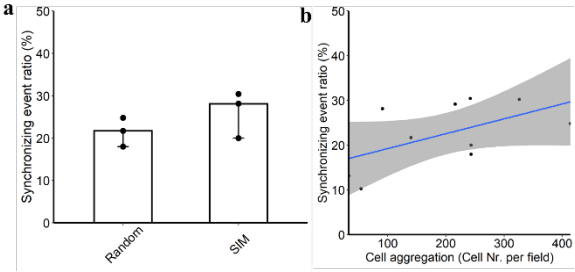

Fig. 3: Multicellular structure by SIM enhanced neuronal synchronization.

ACKNOWLEDGEMENTS: This work is supported by AO foundation.

REFERENCES: [1] D. Petta et al. Biofabrication, **2020**, *v. 13*, 015004; [2] J. Ma et al., Neurospine, **2020**, *v. 17(1)*, p. 42; [3] D. Utzschneider et al., Neuroscience Letters, **1992**, *v. 146(1)*, p. 53.

Effect of Calcium Phosphate Particle Addition on the Properties of Hyaluronic Acid Hydrogels

A. Svarca[1,2], D. Loca[1,2]

[1,2]Rudolfs Cimdins Riga Biomaterials Innovations and Development Centre, Institute of General Chemical Engineering, Faculty of Materials Science and Applied Chemistry, Riga Technical University, Riga, Latvia, [1,2]Baltic Biomaterials Centre of Excellence, Headquarters at Riga Technical University, Riga, Latvia

INTRODUCTION: Hyaluronic acid (HA) is an essential component of the bone extracellular matrix (ECM) as it maintains the viscoelasticity of the ECM and plays a vital role in many biological processes - controls cell-cell and cell-ECM interactions, regulates cell adhesion, proliferation and differentiation. Additionally, as HA has excellent biocompatibility and is completely biodegradable *in vivo*, it is an attractive material for the preparation of hydrogels with the desired morphology and bioactivity [1].

However, HA hydrogels lack of mechanical stability and are rapidly degraded *in vivo* by such enzymes as hyaluronidases. To overcome these shortcomings, HA hydrogels can be modified with an inorganic component of natural bone - calcium phosphate (CaP), thus providing bone-mimetic microenvironment, promoting the bone regeneration and increasing stability of hydrogels [2].

The aim of the current study was to evaluate the influence of inorganic phase (CaP) addition on molecular structure, microstructure, gel fraction and swelling behavior of HA hydrogels. Two different approaches were used for HA/CaP composite preparation – *in situ* CaP synthesis in HA solution and mechanical mixing of CaP and HA. In both prepared composite systems inorganic/organic phase ratio was kept constant.

METHODS: Hydrogels were prepared by mixing all components with 0.25 M NaOH and 1,4-Butanediol diglycidyl ether (BDDE). Obtained systems were crosslinked for 22 h at 45°C, neutralized in physiological solution and lyophilized for 72 h. Prepared samples were used for the determination of gel fraction and swelling degree. Microstructure of obtained samples was evaluated by scanning electron microscopy (SEM). Fourier transform infrared spectroscopy (FTIR) was used to analyze the molecular structure and to determine the possible molecular interactions between components. Additionally, X-ray diffraction analysis (XRD) was performed to assess the crystallinity of raw materials and prepared samples.

RESULTS: Macroporous structure with interconnected pores was observed for all prepared samples. Results indicated that the addition of inorganic phase significantly decreased (up to 4 times) obtained HA/CaP composite swelling degree which could be attributed to the increased (~14%) gel fraction found for CaP modified HA samples. XRD analysis confirmed CaP crystallinity and hydroxyapatite phase was not affected during HA/CaP composite preparation process. Also, the FTIR analysis did not confirm any notable molecular interactions between CaP and HA.

DISCUSSION & CONCLUSIONS: During the research it was established that the properties of HA hydrogels can be tailored by addition of CaP inorganic phase and they also highly depend on the route of nanoparticle introduction into the HA matrix. Taking into the consideration the obtained results, it can be concluded that developed HA/CaP composites are promising materials for bone tissue engineering purposes.

ACKNOWLEDGEMENTS: The authors acknowledge financial support from the Latvian Council of Science project No. lzp-2019/1-0005 “Injectable in situ self-crosslinking composite hydrogels for bone tissue regeneration (iBone)” and support from the European Union’s Horizon 2020 research and innovation program under the grant agreement No 857287 (BBCE).

REFERENCES: [1] P. Zhai et al., Int. J. Biol. Macromol., **2019**, *v. 151(15)*; p. 1224; [2] R. Sikkema et al, Materials, **2021**, *v. 14*, p. 4982.

Biomedical Elastomer for Controlled Drug Delivery

A. Stepulane[1,2], K. Ahlgren[3], M. Andersson[1]

[1]Department of Chemistry and Chemical Engineering, Chalmers University of Technology, Gothenburg, SE, [2]Amferia AB, AZ BioVentureHub, Mölndal, SE ,[3]Department of Physics, Chalmers University of Technology, Gothenburg, SE

INTRODUCTION: Biomedical elastomers play an integral role in manufacturing of medical devices, however, are complicated to endow with function due to material inertness. This study investigates new elastomeric material synthesis by combining polydimethylsiloxane (PDMS) with Pluronic F127 – commonly used biomedical elastomer and amphiphilic hydrogel used in drug delivery systems. New functional elastomers are synthesized with emphasis on drug delivery capacity.
Here, Pluronic F127 has been self-assembled in combination with PDMS and water, producing elastic rubber-like materials of PDMS mechanics with Pluronic F127 capacity to encapsulate and release hydrophobic and hydrophilic therapeutic drugs. Additionally, produced materials are 3D printed in different constructs to demonstrate applicability potential for tailor made medical device production.

METHODS: The materials were synthesized by mixing diacrylate triblock Pluronic F127 copolymers with PDMS prepolymer and water in different compositions according to the Pluronic F127-oil-water ternary phase diagram, and subsequently crosslinked via UV and heat curing [1]. Material mechanical performance was characterized by tensile and compression testing along with structure evaluation with small angle X-ray scattering (SAXS), and material anisotropy investigation with birefringence microscopy. Vancomycin and ibuprofen were chosen as model hydrophilic and hydrophobic drugs, respectively, and their loading and release capacity studied on compositions of interest using UV-Vis spectroscopy. As a proof-of-concept, selected materials were 3D printed to demonstrate the capability of producing functional elastomers of complex architectures.

RESULTS: Analysed compositions of interest constituted homogeneous and tough elastomers with tensile and compressive strength between PDMS elastomer and reference Pluronic hydrogels along with increased elasticity. SAXS data displayed normal micellar cubic structure in all samples without any long-range order. Birefringence microscopy yielded varying results consistent with both, isotropic and anisotropic material structures. Tested composition exhibited sustained release of ibuprofen for 3 – 5 days, and vancomycin for 1 – 6 days, following time dependant zero and first order release pattern (Fig 1.) 3D printing demonstrated the possibility to manufacture complex elastomeric constructs (Fig 1.)

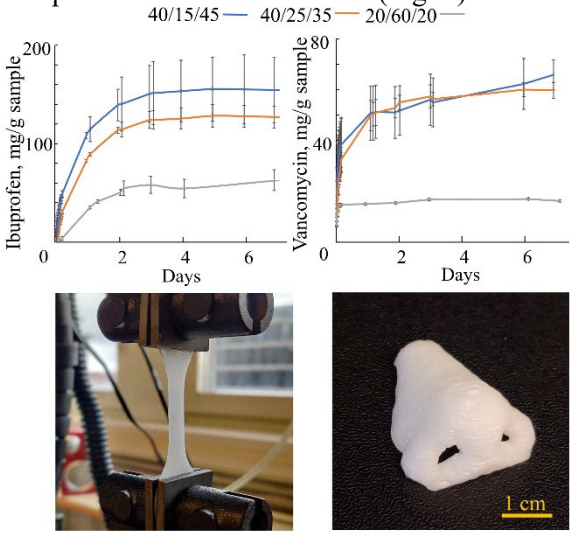

Fig. 1: Top: ibuprofen and vancomycin release from different material compositions (F127/PDMS/H_2O). Bottom: material in strain and 3D printed human nose.

DISCUSSION & CONCLUSIONS: A new class of elastomeric biomaterials have been produced based on combination of PDMS and Pluronic F127. The synthesized elastomers possessed improved mechanical properties with added drug delivery capacity and 3D printability, potentially applicable in drug eluting medical device manufacturing.

ACKNOWLEDGEMENTS: The authors would like to thank the Wallenberg Foundation and the Chalmers Area of Advance “Materials Science” for funding.

REFERENCES: [1] P. Holmqvist et al., J. Phys. Chem., **1998**, *v. 102(7)*, p. 1149.

Adhesive Phosphoserine-Loaded Calcium Phosphate Cements Favour Human Mesenchymal Stromal Cell Mineralisation *In Vitro*

H. Autefage[1], M. Ojansivu[1], M. Pujari-Palmer[2], O. Okude[1], P. Chivers[1], C.D. Spicer[1], H. Engqvist[2], M.M. Stevens[1,3]

[1]*Department of Medical Biochemistry and Biophysics, Karolinska Institutet, Stockholm, SE,* [2]*Applied Material Science, Department of Engineering, Uppsala University, Uppsala, SE,* [3]*Department of Materials, Department of Bioengineering, Institute of Biomedical Engineering, Imperial College London, London, UK*

INTRODUCTION: We have recently demonstrated that the addition of phosphoserine (PSer) to alpha-tricalcium phosphate (α-TCP) bone cements confer to the material strong adhesive properties, allowing us to rapidly and firmly bond various synthetic and biologically-derived materials together [1-3]. This groundbreaking discovery has the potential to drastically facilitate the next generation of orthopaedic and dental clinical practices. *In vitro* and *in vivo* characterisations [4] are a key requirement in the clinical translation process of newly developed biomaterials, as they provide data on the materials' biocompatibility and biological performances over time. Here, we hypothesized that the addition of the calcium phosphate-nucleating agent PSer into well-established α-TCP-based bone cements would allow human mesenchymal stromal cell (hMSC) proliferation and favour their osteogenic differentiation.

METHODS: Apatitic calcium phosphate bone cement disks were prepared using α-TCP as a precursor, in absence or presence of PSer or control L-serine (L-Ser). The cement composition and adhesive properties were assessed by X-ray diffraction and shear strength measurements, respectively [1], [2]. The cements' *in vitro* biocompatibility and osteogenic properties were assessed following direct and indirect culture with hMSCs for up to 21 days in media supplemented with osteogenic agents. Human MSC viability, proliferation, osteogenic differentiation were assessed using biochemical assays and confocal microscopy.

RESULTS: α-TCP-based cements containing PSer were found to have strong adhesive properties compared to L-serine and unloaded control cements [1,2]. Following curing, a significant amorphous phase was detected in the PSer-loaded cements. hMSCs were found to adhere and proliferate on Pser-containing cements as well when in contact with their conditioned media, as demonstrated by AlamarBlue™ metabolic activity and Picogreen assays, and imaging of phalloidin-AF647/DAPI staining. Alkaline phosphatase activity (ALP) was markedly increased in hMSCs after 7 and 14 days of direct and indirect contact with cements loaded with 50 mol% of PSer. Human MSC matrix mineralisation similarly significantly increased when the cells were incubated with PSer-containing cement conditioned media, suggesting a direct contribution of PSer upon release from the cements.

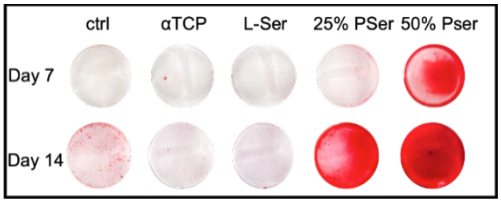

Fig. 1: Alizarin Red S staining of calcium deposition in hMSCs cultured in PSer-loaded or control cement-conditioned media in presence of osteogenic agents.

DISCUSSION & CONCLUSIONS: We have demonstrated that Pser-containing calcium phosphate cements not only had strong adhesive properties, but also allowed hMSC proliferation and supported their osteogenic differentiation as reported by an increased ALP activity and mineralisation *in vitro*. This study provides new important information on the interactions of the novel material with osteoprogenitor cells *in vitro*.

ACKNOWLEDGEMENTS: This work was supported by the Swedish Science Foundation (#RMA15-0110).

REFERENCES: [1] M. Pujari-Palmer et al., Materials, **2018**, *v. 11(12)*, p. 2492; [2] C.D Spicer et al. ACS Cent. Sci., **2020**, *v. 6(2)*, p. 226; [3] R. Mathew et al., J. Phys. Chem. C, **2020**, *v. 124(39)*, p. 21512; [4] H. Autefage et al., Biomaterials, **2019**, *v. 209*, p. 152.

Influence of Bioactive Glass Particle Size on Setting Time, Mechanical Properties and *In Vitro* Biocompatibility of Calcium Phosphate Bone Cements

Ö. Demir-Oğuz[1,2], A.R. Boccaccini[3], D. Loca[1,2]

[1]Rudolfs Cimdins Riga Biomaterials Innovations and Development Centre of RTU, Institute of General Chemical Engineering, Faculty of Materials Science and Applied Chemistry, Riga Technical University, Riga, Latvia, [2]Baltic Biomaterials Centre of Excellence, Headquarters at Riga Technical University, Riga, Latvia, [3]Institute of Biomaterials, Department of Materials Science and Engineering, University of Erlangen-Nuremberg, Erlangen, Germany

INTRODUCTION: Apart from being injectable, calcium phosphate bone cements (CPCs) exhibit notable biocompatibility and osteoconductivity [1]. Nevertheless, CPC possess slow degradation rate within the body which should be further improved and well-balanced to the dynamics of new bone formation. Additionally, the osteoconductive properties of CPC might not be adequate to induce bone healing in critical or non-union bone defects. Bioactive glasses (BGs) are well-known for their direct bone bonding ability as well as their high bioactivity, which make them good candidates to enhance drawbacks of CPCs [2]. In this context, combination of CPCs and BGs is a practical approach that provides the possibility to develop CPC/BG composites with adequate mechanical properties, biomimetic interface and enhanced cell attachment and differentiation. Within the current research the effect of different size BG particle incorporation into the CPC matrix was explored and CPC/BG composites were characterized towards their physicochemical and *in vitro* biocompatible properties.

METHODS: 58S BG powder with a composition of $58SiO_2$-$33CaO$-$9P_2O_5$ (wt.%) was prepared by sol-gel technique and calcined for 3 hours at 700 °C. BG powders with different particle size (20, 38 and 100 µm) were used (7wt% and 9wt%) in a combination with α-TCP powder to prepare CPC/BG composites. Setting time of prepared cements was measured using Gillmore needle. Compressive strength of CPC/BG composites was determined after their complete setting by using universal testing machine at crosshead speed of 1mm/min. *In vitro* biocompatibility of MG63 cells on extracted medium (at day 1,3 and 7) of CPC/BG composites was assessed using WST-8 assay.

RESULTS: Obtained results revealed that BG addition increased the CPC setting time. Moreover, increase of BG particle size led to the setting time decrease (from 38.17 ± 0.05 (20 µm) to 7.96 ± 0.09 min (100 µm), if 7wt% of BG was used and from 115.35 ± 0.13 (20 µm) to 10.17 ± 0.09 (100 µm), if 9wt% of BG was used). Influence of BG addition on CPC mechanical properties was determined. It was found that after the final setting of CPC/BG composite cements compressive modulus decreased for more than 4 times in case of CPC/BG composites with 9wt% of 100µm BG particles. *In vitro* biocompatibility of all prepared CPC/BG compositions was assessed using MG63 cells. Obtained results confirmed that despite of different CPC/BG compositions cell viability was >90% for all tested samples.

DISCUSSION & CONCLUSIONS: Summarizing the obtained results it was concluded that BG particle size matters and has a great influence not only on the CPC/BG composite setting time, but also on cement mechanical properties, suggesting that more in-depth investigations should be performed to analyse the CPC/BG microstructure and behaviour in biological fluids.

ACKNOWLEDGEMENTS: The authors acknowledge financial support from the European Union's Horizon 2020 research and innovation programme under the grant agreement No 857287 (BBCE).

REFERENCES: [1] [S. V Dorozhkin et al., Angew. Chem. Int. Ed. Engl., **2002**, *v. 41*, p. 3130; [2] M. Karadjian et al., Int. J. Mol. Sci., **2019**, *v. 20*, p. 1.

Composite Scaffolds Based on β tricalcium Phosphate and Poly(3-hydroxybutyrate) for Bone Tissue Regeneration

A. Zima[1], J.P. Czechowska[1], S. Skibiński[1], E. Cichoń[1], P. Pańtak[1], M. Guzik[2], A. Ślosarczyk[1]

[1]Faculty of Materials Science and Ceramics, AGH University of Science and Technology, Krakow, Poland, [2]Jerzy Haber Institute of Catalysis and Surface Chemistry Polish Academy of Sciences, Krakow, Poland

INTRODUCTION: Calcium phosphates (CaPs), due to their biocompatibility and bioactivity, have been successfully used as bone grafts. In the case of macroporous CaPs materials the main drawback is the difficulty in achieving adequate mechanical strength. The combination of bioresorbable scaffolds (i.e. β tricalcium phosphate (β-TCP)) with degradable polymers not only may lead to the improvement of mechanical properties, but also can provide a sustained and controlled release of drugs or bioactive molecules supporting tissue regeneration [1,2]. However, in some cases, it is difficult to obtain a uniform and stable polymer coating on the ceramic surface. The polyhydroxyalkanoates (PHAs) represent a class of polyesters of bacterial origin, which may be applied as a coating on bioceramic scaffold. Poly(3-hydroxybutyrate) (P(3HB)) is an example of biocompatible and biodegradable polyhydroxyalkanoates. In this study, we used P(3HB) as a coating on β-TCP scaffolds. The pre-treatment with the citric acid was made to enhance bonding between ceramic surface and polymer layer in composites. The influence of the P(3HB) coating on physicochemical properties of materials has been investigated.

METHODS: β-TCP scaffolds were fabricated by a foam replication method using three types of polyurethane matrices with different pore sizes (S-small, M-medium, L-large). Foams were impregnated in slurry (composed of β-TCP powder, Dispex A4040, distilled water, and methylcellulose), dried and sintered at 1150 °C. Afterwards, bioceramic scaffolds (non-treated (TCP) and treated with citric acid (eTCP)) were soaked in the P(3HB) solution, dried and subjected to further studies. Obtained materials were assessed by X-ray diffraction, scanning electron microscopy, hydrostatic weighing, compression tests and chemical stability *in vitro*. Degradation products of P(3HB) were analyzed via UHPLC-MS.

RESULTS: XRD studies confirmed that the scaffolds composed of only one crystalline phase *i.e.* β-TCP and amorphous halo originated from the polymer. SEM observations of the composites (Fig. 1) demonstrated macroporous microstructure with improved adhesion of P(3HB) film to the pre-treated β-TCP scaffolds (eTCP/P(3HB)).

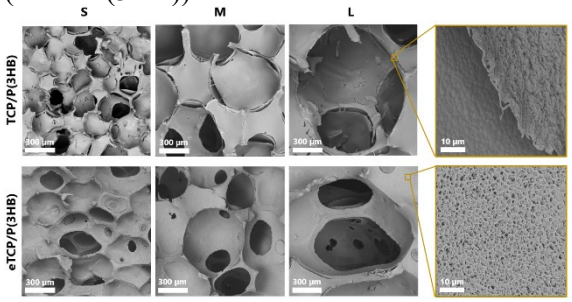

Fig. 1: Microstructure of the obtained composites.

eTCP/P(3HB) composites possessed higher comprehensive strength (up to 4.5±0.5 MPa) in comparison to TCP/P(3HB) scaffolds (up to 3.2±0.5 MPa). Studied materials were chemically stable and did not show significant pH fluctuations during 28 days of incubation in SBF. *(R)*-3-hydroxybutyric acid and its oligomers were identified as P(3HB) degradation products.

DISCUSSION & CONCLUSIONS: Etching with citric acid increased the surface roughness of the β-TCP, what led to the increase in adhesion of P(3HB) coating and the improvement in the mechanical properties of the composites. Moreover, P(3HB) degradation products may act as the nourishing agents for surrounding tissues [3].

ACKNOWLEDGEMENTS: Research funded by the National Centre for Research and Development, Poland, grant Techmatstrateg no. TECHMATSTRATEG2/407507/1/NCBR/2019

REFERENCES: [1] A. Philippart, et al., Exp. Rev. Med. Devices, **2015**, *v. 12(1)*, p. 93; [2] E. Cichoń, et al., J. Mech. Behav. Biomed. Mater., **2019**, *v. 98*, p. 235; [3] S. Cheng et al., Biomacromolecules, **2005**, *v. 6(2)*, p. 593.

Low Temperature Synthesis and Cold Sintering of Nano-hydroxyapatite for Biomedical Applications

A. Galotta[1], F. Agostinacchio[1,2], A. Motta[1,2], S. Dirè[1], V.M. Sglavo[1]

[1]Department of Industrial Engineering, University of Trento, Trento, IT, [2] BIOTech Research Center, Department of Industrial Engineering, University of Trento, Trento, IT

INTRODUCTION: The cold sintering process (CSP) is an attractive and innovative technique able to satisfy the increasing demand for a fast and low-energy consuming process in agreement with the *green economy* perspective. CSP allows to consolidate materials at a temperature below 350 °C [1] with the application of an external pressure during heating, and it allows to sinter materials undergoing phase transformation at high temperature such as hydroxyapatite (HAp). HAp is a bioactive, osteoconductive, osteointegrative calcium phosphate and is one of the most studied bioceramic since its chemical composition resembles the mineralized part of bone tissue. In this work, discarded mussel shells are exploited as a biogenic source of calcium carbonate for the production of ion-substituted hydroxyapatite powders. HAp is synthesised at room temperature via mechanochemical route, and it is consequently consolidated by cold sintering process (CSP) to produce scaffolds suitable for bone tissue regeneration.

METHODS: Hydroxyapatite nano-powders were produced via mechanochemical synthesis at room temperature, by mixing a phosphoric acid solution with discarded mussel shells, previously cleaned and crushed [2]. The as-synthesized powder was analysed by X-ray diffraction (XRD), inductively coupled plasma optical emission spectroscopy (ICP-OES), field emission scanning electron microscopy (FE-SEM) and Fourier-transformed infrared spectroscopy (FT-IR). HAp was then consolidated at low temperature (200°C) by cold sintering. The powder was first mixed with 0.1 M EDTA solution and then it was pressed up to 600 MPa and simultaneously heated up to 200 °C. Sintered samples were characterized by XRD, SEM, densimetry. Mechanical and biological investigation were also carried out on sintered pellets.

RESULTS & DISCUSSION: Pure nanocrystalline HAp powder was consolidated up to a relative density (RD) of ~85% by cold sintering. The XRD and FTIR spectrum of sintered bodies did not show any change in the material with respect to the as-synthesised powder. During CSP, pressure provides the main driving force for densification but a significant improvement in terms of density was not observed above 500 MPa. A net increase in relative density was observed moving from dry (~75%) to wet condition (~85%). A holding time longer than 15 min did not provide any increase in relative density. Therefore, material consolidation is triggered by the presence of the solvent: once the liquid evaporates, densification stops. Nevertheless, a temperature increase from room temperature to 200 °C also enhanced densification. Cold sintered HAp samples showed a flexural strength comparable to commercial HAp sintered at 1200 °C. Moreover, the in vitro assessment showed a good cell viability in terms of adhesion and proliferation of human bone marrow-derived mesenchymal stem cells.

CONCLUSIONS: Cold sintering allows to strongly reduce energy, time and costs in comparison with traditional sintering techniques. Nano-HAp was successfully sintered above 80% of relative density at 200 °C in about 15 min. Pressure plays the major role during CSP but also the liquid phase and temperature affect material consolidation. Cold-sintered HAp showed promising mechanical and *in vitro* results as scaffolds for bone tissue regeneration.

ACKNOWLEDGEMENTS: This work was supported by the Italian Ministry of University and Research (MIUR) within the “REGENERA” and “E-Mat” projects of the Departments of Excellence 2018–2022 (DII-UNITN) program.

REFERENCES: [1] J. Guo et al., Annual Review of Materials Research, **2019**, *v. 49*, p. 275; [2] F. Cestari et al., Ceramics International, **2020**, *v. 46*, p. 23526.

How Thermal Degradation of the Polymeric Matrix Influence the Phase Composition of Bioceramic Scaffolds?

E. Cichoń[1], J. Czechowska[1], S. Skibiński[1], P. Pańtak[1], A. Ślósarczyk[1], A. Zima[1]

[1]*Faculty of Materials Science and Ceramics, AGH University of Science and Technology, Krakow, Poland*

INTRODUCTION: The polymer matrix replication is one of the methods used to obtain porous scaffolds. It is known that the architecture of the foam has a direct influence on the architecture of the final sinter. However, little attention has been paid to the chemical composition of the matrix and its influence on the thermal processing of ceramic materials. This study aimed to compare the phase composition of ceramic scaffolds obtained using two different polyurethane sponges in the context of the processes occurring in the matrix itself during the thermal treatment of the materials.

METHODS: In order to obtain highly porous scaffolds two types of polyurethane sponges (I-Bulpren, II-Eurofoam) were soaked in β-tricalcium phosphate-based (β-TCP) ceramic slurry, dried at 60°C and sintered at 1200°C. The phase composition of both types of scaffolds was determined via XRD method and compared. Additionally, the process of thermal decomposition of the applied polyurethane matrices was studied by thermal analysis method combined with the examination of decomposition products (DSC-TG-MS).

RESULTS: TG-DSC curves are shown in Fig. 1. In the thermogravimetric curve (TG), the mass loss of the polyurethane sponge during heating can be observed. The greatest weight loss is seen in the temperature range 250-650 °C (with maxima at 275 °C and 322 °C) when degradation of the so-called flexible segments occurs. Above 700°C, no further decrease in sample mass can be seen. In the case of sponge I the amount of the organic residue formed during the combustion of the matrix was 6.6% of its initial mass, whereas for sponge II it was 17.5%. The XRD analysis revealed that the scaffold obtained from sponge I composed of 97-99 wt% of β-TCP and 1-3 wt% of α-TCP, whereas scaffold II consisted of 77-88 wt% of β-TCP and 12-23 wt% α-TCP. The difference in the phase composition was most likely due to the release of various amounts of gases during the burning of the matrices I and II and the presence of organic residues.

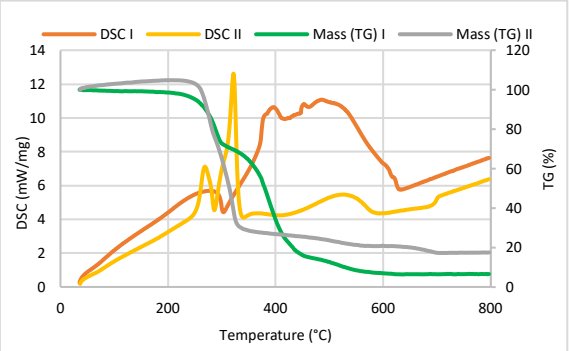

Fig. 1: TG-DSC curves for combustion of polyurethane matrices used for bioceramic scaffolds fabrication.

DISCUSSION & CONCLUSIONS: The mechanism of thermal degradation of polyurethanes is described in the literature as a very complex process, which involves dissociation of the initial components: polyol and isocyanate, followed by thermal decomposition leading to the formation of carbon oxides (CO_2, CO), water (H_2O), nitrogen oxides (NOx) and hydrogen cyanide (HCN)[1,2]. Presumably, the releasing gases and organic residues influenced the thermal transformation of the tricalcium phosphate as in the case of using sponge II (Eurofoam) for scaffold fabrication more α-TCP was present in the final material.

ACKNOWLEDGEMENTS: Research funded by the National Center for Research and Development, Poland, grant Techmatstrateg no. TECHMATSTRATEG2/407507/1/NCBR/2019. E.C. acknowledges financial support from the National Science Centre, Poland under Doctoral Scholarship No. 2019/32/T/ST5/00207

REFERENCES: [1] K. Voorhees et al., J. Polym. Sci. Part A, **1978**, *v. 16*, p. 213; [2] T. Rogaume et al., Combustion Science and Technology, **2011**, *v. 183(7)*, p. 627.

Silk Fibroin Conduits Made with Aligned Nanofibres for Peripheral Nerve Regeneration

D. Torres Ulloa[1], J.J. Blaker[1,2]

[1]Department of Materials and Henry Royce Institute, The University of Manchester, Manchester M13 9PL, United Kingdom, [2]Department of Biomaterials, Institute of Clinical Dentistry, University of Oslo, Oslo, Norway

INTRODUCTION: Autografts, the gold standard therapy for peripheral nerve injuries, require donor tissue and a second incision. Peripheral nerves have some regenerative capacity, which could be enhanced by nerve guidance conduits. Such conduits should provide topographic and biological cues to guide nerve regrowth from the proximal to the distal end of the injured nerve. Nanofibrillar conduits have been explored to provide guidance cues. In this work nanofibre yarn spinning and macro-fibre overcoating has been used to give control over fibre orientation and enable multiple channel nanofibre conduits.

METHODS: Silk fibroin cast films were dissolved in HFIP to obtain 6% w/v solutions. These solutions were electrospun (±13 kV, 20 cm working distance, 4 mL/h in each of two syringes) using a custom-built yarn module to overcoat sacrificial macro-fibre yarns (polyvinyl alcohol (PVA) or phosphate glass fibres – PGF). The composite threads were treated with 80% ethanol for 20 minutes, water-quenched, and then submerged into an appropriate solvent to dissolve the sacrificial fibres to give silk conduits with controlled nanofibre fibre alignment.

RESULTS: Nanofibres alignment degrees of near zero were obtained relative to the axis of the sacrificial fibre. The finished construct depends on the reeling speed of the thread and the application of tension while water-quenching. The angle at which the nanofibres are oriented can be modified by faster reeling of the thread, with faster speeds producing a smaller fibre-to-thread angle. Dry, ethanol treated silk threads behave in a more brittle way than in the wet state, where strains of at least 65% were reached without failure. Microchannels of various sizes (ranging from 100 to 250 µm) were obtained and the channel size depends on the diameter of the sacrificial thread substrate.

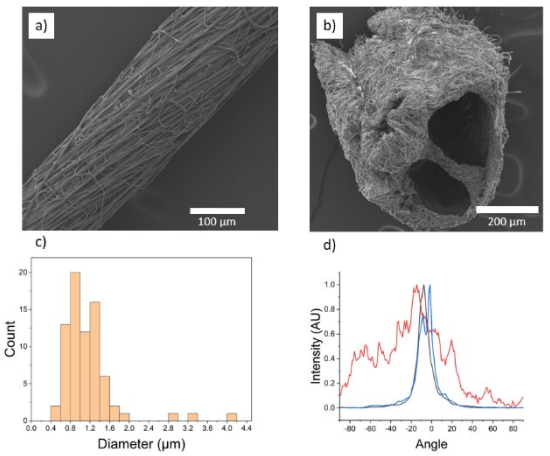

Fig. 1: Silk guidance conduits. a) Nanofibrous silk thread with nanofibres oriented towards the thread axis. b) Multi-channel nanofibrous nerve guidance conduit. c) Diameter of silk nanofibres on a PVA thread substrate. d) Orientation of silk nanofibres relative to the thread axis after different treatments: Blue: as spun; black: ethanol under tension, and red: ethanol treated with no tension applied.

DISCUSSION & CONCLUSIONS:
Mechanical properties and surface morphology appear suitable for nerve tissue regeneration applications; the inner diameter size is suitable for the growth of nerve bundles according to literature[1]. Different substrates (PVA, PGF) can be coated by this method and different substrates can have different applications. The phosphate based glass has potential as an *in situ* porosifier and can release stimulatory ions.

ACKNOWLEDGEMENTS:
Agencia Nacional de Investigación y Desarrollo (ANID) for funding. And to Prof. Jonathan Knowles (UCL) for providing the PGF.

REFERENCES: [1] S. Song et al., Front. Bioeng. Biotechnol., **2020**, *v. 8*, 590596.

A Universal Microfluidic Platform for *In Vitro* Biomaterial Evaluation

Abdul Raouf Atif[1], Sarah-Sophia Carter[1], Hanlu Deng[1], Håkan Engkvist[1], Maria Tenje[1], Gemma Mestres[1]

[1]*Departament of Materials Science and Engineering, Science for Life Laboratory, Uppsala University, Uppsala, Sweden*

INTRODUCTION: Conventionally, the biological properties of biomaterials are evaluated using well plates. Although being a standardized method, it is static in terms of fluid flow and is far from the physiological conditions found *in vivo*. This work presents a versatile microfluidic system that allows for integration of different biomaterials (ceramic, metals and polymers) under dynamic conditions.

METHODS: The Universal Biomaterial-on-Chip (UBOC) consisted of two separate 3D printed (Polylactic acid, Ultimaker 2+) structures: the upper layer which contains the channel through which medium can flow (Fig 1A) and the bottom layer that holds and secures the biomaterial in place (Fig 1B). A glass coverslip was taped to the upper layer to tightly seal the channel. Subsequently, an oval Polydimethylsiloxane (PDMS) gasket (l=10mm, w=7mm, h=0.8mm) was inserted into the periphery of the channel in the upper layer. Furthermore, magnets (Ø=12mm, h=3mm) were glued on both sides of the bottom layer. To close the channel, two magnets were placed on the upper layer, causing attraction to the magnets in the bottom layer. The gasket would then directly interface with the biomaterial inside the bottom layer, creating a leak-free channel on its surface. MC3T3-E1 pre-osteoblasts were seeded in the UBOC platform (50,000 cells/cm^2) on calcium-deficient hydroxyapatite (HA) (Ø=15mm) and clinical grade titanium (Ti) (Ø=12mm). The cells were cultured for a period of 5 days at a flow rate of 2 µl/min using supplemented MEM-α medium (Hyclone, 10% FBS, 1% Pen-Strep). On day 5, the cells were stained on-chip with Live/Dead stain (Calcein, Propidium Iodide and Hoechst) and subsequently imaged.

RESULTS: HA and Ti samples were successfully integrated into the UBOC. Cells cultured on-chip displayed a high degree of viability and confluence on day 5 of culture on both HA and Ti substrates (Fig 2).

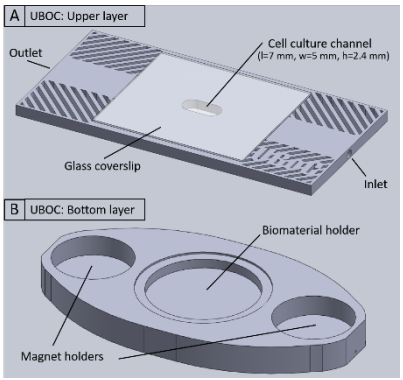

Fig. 1: 3D model for A) Upper and B) Lower layer of UBOC.

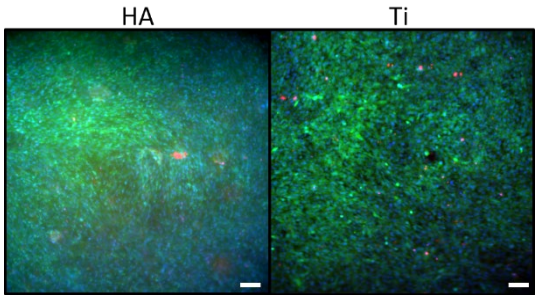

Fig. 2: MC3T3 culture on HA and Ti substrates in UBOC after 5 days (Scale bar is 100 µm).

DISCUSSION & CONCLUSIONS: UBOC presents the possibility for flexible *in vitro* biomaterial analysis as it allows for easy incorporation of flow to conventional cell culture regimes in a low-cost manner. Via this method, cells can be cultured on the biomaterial with exposure to fluid flow and controlled shear-stress. The platform is compatible with standard characterization methods, such as imaging and biochemical cell analysis. In addition, since the system is designed to be opened and closed, the biomaterial could be easily accessed, harvested and transferred to a regular tissue culture vessel, enabling standard off-chip biochemical assays and protocols to be performed for further analysis.

ACKNOWLEDGEMENTS: G. Mestres acknowledges VR (2017-05051), and Göran Gustafsson's Foundation (2021-2126) for financial support.

Engineered Calcium Phosphate Nanoparticles: A Novel Platform for Drug Delivery

V. Tsikourkitoudi[1], GA. Sotiriou[1]

[1]*Department of Microbiology, Tumor and Cell Biology, Karolinska Institutet, Stockholm, Sweden*

INTRODUCTION: Nanomedicine has gained considerable attention recently and nanoparticle-based drug delivery systems are rapidly evolving to improve treatment for various diseases. Most of the nanoparticle-mediated treatments approved for clinical use nowadays are using liposomes as drug carriers. Although various novel materials have been tested as drug delivery agents, there is still a long way from their demonstration in the laboratory until their large quantity production with reproducible properties that is necessary for their clinical use [1]. In this regard, here we propose a novel drug delivery platform based on calcium phosphate (CaP) nanoparticles. We fabricate the nanoparticles by flame spray pyrolysis (FSP) that is a nanomanufacturing process famous for its scalability and reproducibility and assess their therapeutic potential against bacterial infections.

METHODS: We extensively characterize the as-synthesized CaP nanocarriers in terms of their physicochemical properties, *i.e.*, specific surface area/size, crystal phase, crystallinity, and colloidal stability. We further establish an experimental protocol for loading biologics on flame-made CaP nanoparticles and evaluate their antimicrobial activity. More precisely, we load antimicrobial peptides (LL-37 and a mannose receptor-derived one) on CaP by physisorption and evaluate their stability against proteolytic degradation and their antimicrobial performance upon loading *in vitro* and *in vivo*.

RESULTS & DISCUSSION: High peptide loading values are obtained that guarantee low nanocarrier dose for flame-made nanoparticles. Physisorption of LL-37 on CaP protects the peptide from enzymatic degradation and does not affect its antimicrobial functionality against both Gram-positive (*Streptococcus pneumoniae*) and Gram-negative (*Escherichia coli*) pathogens [2]. Typical fractal-like structure of agglomerated/aggregated nanoparticles made by FSP promotes high drug loading efficiency and enables the protection of the drug from enzymatic degradation, enabling its safe delivery [3].

Mannose receptor derived (MRC-1) peptide loaded CaP nanoparticles were administered intranasally to mice previously infected by *S. pneumoniae.* They are shown to reduce development of pneumococcal disease *in vivo* enhancing mice survival [4].

CONCLUSIONS: In a nutshell, we present nanocarrier synthesis by FSP, an intrinsically scalable and reproducible nanoparticle synthesis method. High loading values achieved along with the *in vitro* and *in vivo* protective effect of the nanoparticles facilitate clinical translation of flame-made CaP nanoparticles as drug carriers.

ACKNOWLEDGEMENTS: This work was supported by European Research Council (ERC) under the European Union's Horizon 2020 research and innovation program (ERC Grant agreement n° 758705). Funding from Karolinska Institutet Board of Research, Swedish Research Council (2016-03471; 2016- 00228; 2016-01861; 2018-05798), Jeansson Foundations (JS2016-0029), Torsten Söderberg Foundation (M87/18), and the Swedish Foundation for Strategic Research (FFL18-0043) is kindly acknowledged.

REFERENCES: [1] P. Grodzinski et al., ACS Nano, **2019**, *v. 13*, p. 7370; [2] V. Tsikourkitoudi et al., Molecules, **2020**, *v. 25*, p. 1747; [3] F.H.L. Starsich et al., Annu. Rev. Chem. Biomol. Eng., **2019**, *v. 10*, p. 155; [4] K. Subramanian et al., EMBO Mol. Med., **2020**, e12695.

Composite Culture Substrate for Osteoblast Differentiation Made from Beta-Tricalcium Phosphate and Collagen

J.T. Koivisto[1], C. Oelschlaeger[2], D. Menne[2], N. Willenbacher[2], T. Näreoja[1,3]

[1]Department of Laboratory Medicine, Karolinska Institutet, Stockholm, Sweden, [2] Institute of Mechanical Process Engineering and Mechanics, Karlsruhe Institute of Technology, Karlsruhe, Germany, [3] Department of Life Technologies, University of Turku, Turku, Finland

INTRODUCTION: Development of *in vitro* bone disease models is needed for biomarker discovery in diseases such as inflammatory osteolysis. To study the osteoblast function in 3D culture, we focused on the changes in physical properties, primarily using multiple particle tracking microrheology and Voronoi diagrams to quantify the change in substrate mechanics around cells. Beta-tricalcium phosphate (β-TCP) scaffold was prepared from optimized ternary capillary suspension ink, yielding structure with >65% strut porosity and surface roughness suitable for cell attachment. The scaffold was filled with TeloCollagen®, a hydrogel produced by acid-extraction method.

METHODS: Mouse origin MC3T3-E1 pre-osteoblasts were cultured in osteogenic differentiation medium, inside 3D constructs prepared by direct ink writing of β-TCP scaffold and filled with TeloCollagen® (3mg/ml & 6mg/ml) hydrogel and cells (at $5*10^6$ cell/ml concentration). Polystyrene tracer particles with FITC-functionalization were added to enable microrheology. Samples (n>3) were measured on days 0, 4 and 7 using microrheology, bulk rotational rheometry and uniaxial compression.

RESULTS: Microrheology shows tracer particles either elastically trapped or freely moving in viscous liquid. During culture the amount of tracers with viscous behaviour increased, degradation of the matrix releasing the previously elastically trapped particles. This was most rapid in 3mg/ml TeloCollagen® with β-TCP scaffold. The same effect was seen, but to a lesser degree, with higher TeloCollagen® concentration or without the β-TCP scaffold. Without cells present, no degradation of the matrix occurred.
Complementary macroscale measurements reveal first a small reduction of matrix stiffness (plateau modulus) on day 4 and then slight rise in stiffness of bulk sample again at day 7.

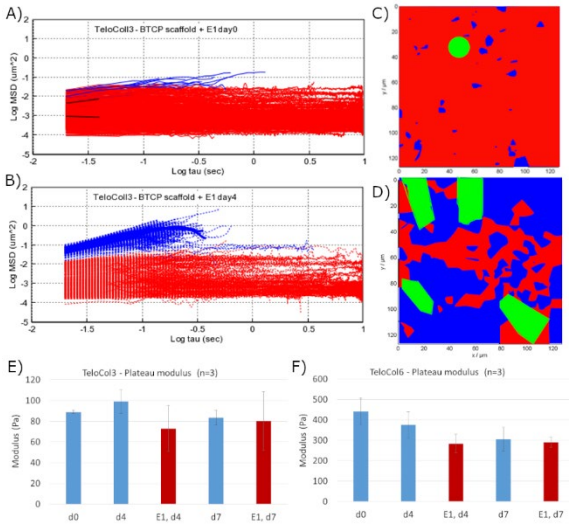

Fig. 1. Mean-square displacements of tracer particles obtained at days 0 (A) and 4 (B). Corresponding Voronoi diagrams shown in (C) and (D), with red area indicating elastic and blue viscous behaviour, and green the cell positions. Growth of viscous area indicates matrix degradation caused by cells. Macro-rheology shows drop of bulk plateau modulus for both TeloCollagen concentrations (E & F).

DISCUSSION & CONCLUSIONS: Rapid remodelling of hydrogel matrix was seen at day 4 in microscale, especially with β-TCP scaffolds in the lower collagen concentration. Bioactivating effect of β-TCP requires optimal matrix stiffness and/or porosity to reach full potential. Additionally, the microrheology with Voronoi diagrams is shown to be a powerful tool to study rapid changes in microstructural (porosity) and micro-mechanical properties in hydrogel-based samples at cell-relevant scales throughout the culture period.

ACKNOWLEDGEMENTS: We wish to thank Prof. Dr. Martin Bastmeyer, Cell- and Neurobiology, Karlsruhe Institute of Technology, for access to cell culture facilities and Osk. Huttunen Foundation for financial support of this research project.

Hydrogel/Nanoparticle Composites as Cheap and Versatile Biosensors

P.R.A. Chivers[1], I. Baldassarri[1], D. Chatzikosmidou[1], M.M. Stevens[1,2]

[1] *Institutionen för Medicinsk Biokemi och Biofysik, Karolinska Institutet, Stockholm, SE,* [2]*Department of Materials, Department of Bioengineering, Institute of Biomedical Engineering, Imperial College London, London, UK*

INTRODUCTION: The development of cheap yet sensitive technologies for the detection of disease biomarkers is of great importance. Gold nanoparticles (AuNPs) are widely cited as effective materials for colorimetric sensors [1], but issues with long-term stability alongside the need for toxic reagents and specialized detection equipment [2] have limited their utility in point-of-care diagnostic devices. Here we demonstrate that simple, self-assembled gels formed from protected amino acids [3] act as both reducing agent and stabilizer for AuNPs, promoting their formation, and enabling long-term storage and assay sensitivity comparable to or superior to commercial alternatives.

METHODS: Coupling of 9-anthraldehyde to amino acids yielded gelators Anth(Trp), Anth(Tyr) and Anth(Phe). Gels containing up to 5 mM AuNPs were formed by mixing a solution of gelator in DMSO with aqueous $HAuCl_4{\cdot}3H_2O$ at a 9:1 v/v ratio. Formation of AuNPs was assessed by UV-vis spectroscopy and scanning electron microscopy. Mechanical properties of the gels were measured by rheology. Gel/AuNP cytotoxicity towards HeLa cells and hMSCs was evaluated *via* Live/Dead staining and alamarBlue™ assay up to 7 days post-seeding. Gel/AuNP composites were cast in 96-well plates (50 µL) and treated with (i) TMB·2HCl (5 mM) and H_2O_2 (0.1-20 mM) to assess catalase-like activity; or (ii) L-serine or L-cysteine (0.06-1 mM) to test for thiol sensing.

RESULTS: Hydrogels formed from all three gelators but only Anth(Trp) and Anth(Tyr), with reducing groups in the amino acid side chain, stimulated formation of AuNPs within the gel matrix. The presence of AuNPs was confirmed by the diagnostic surface plasmon resonance (SPR) peak at 546 nm as well as by SEM (*Fig. 1)*. The presence of AuNPs did not significantly affect gel mechanical properties, nor did they induce significant cell death.

The hydrogel/AuNP materials were found to act as effective catalase/peroxidase mimics, catalyzing the decomposition of hydrogen peroxide. Concomitant oxidation of TMB allowed quantification of H_2O_2 concentration at micromolar levels. The composites were also effective for thiol sensing. Using cysteine as a model analyte, colour changes resulting from thiol-induced aggregation were visible to the naked eye at concentrations ≤ 60 µM. The sensitivity and selectivity of both assays were tuned by altering NP concentration and gel pH.

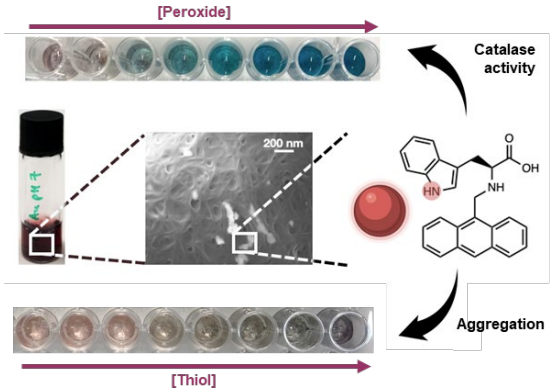

Fig. 1: Self-assembled hydrogels promote the formation of stable AuNPs, which demonstrate colorimetric sensing through enzyme-mimicking activity and thiol-induced aggregation.

DISCUSSION & CONCLUSIONS: We have prepared cheap and synthetically accessible AuNP-based biosensors through encapsulation in a self-assembled hydrogel matrix. The gel/NP composites show sensing capabilities similar to peroxidase-based assays, and exceeding those of many commercial assays for thiols (e.g. Ellman's). The composites are stable over several months, making them viable materials for further testing in more challenging media and for detection of more biologically relevant analytes; a key focus of future work.

ACKNOWLEDGEMENTS: We acknowledge Wenner-Gren Foundation for PRAC's research fellowship and Erasmus+ for IB's internship. We thank Dr. Fei Ye (KTH, SV) for SEM.

REFERENCES: [1] H. Aldewachi et al., Nanoscale, **2017**, *v. 10*, p. 18; [2] R. de la Rica and M.M. Stevens, Nat. Nanotechnol., **2012**, *v. 7*, p. 821; [3] P.R.A. Chivers et al, Chem. Commun., **2020**, *v. 56*, p. 13792.

Biocompatible Gallium Doped Hydroxyapatite

M. Mosina[1,2], C. Siverino[3], L. Stipniece[1,2], F. Moriarty[3], J. Locs[1,2]

[1]Rudolfs Cimdins Riga Biomaterials Innovations and Development Centre of RTU, Institute of General Chemical Engineering, Faculty of Materials Science and Applied Chemistry, Riga, Latvia, [2] Baltic Biomaterials Centre of Excellence, Headquarters at Riga Technical University, Riga, Latvia, [3]AO Research Institute Davos, Switzerland

INTRODUCTION: Biomaterial implantation has a high risk of infection. Additionally, bacterial antibiotic resistance increases every year representing one of the biggest threats to global health. Gallium has shown antibacterial activity against different bacterial strains. Therefore, gallium doped hydroxyapatite (GaHAp) could be used as antibacterial agent. The aim of the study was to investigate the effect of gallium on hydroxyapatite properties and the GaHAp effects on human fibroblasts viability.

METHODS: GaHAp was synthesized with wet chemical precipitation method with concentration of gallium 2wt%, 4wt%, 6.3wt% and 8wt%. CaO, H_3PO_4 and $Ga(NO_3)_3$*xH_2O were used as raw materials. Synthesis was performed at 45 °C and final pH was 6.95±0.05. GaHAp was characterized with X-ray Diffraction analysis (XRD), Fourier Transform Infrared Spectroscopy (FTIR) and Specific Surface Area (SSA) was measured with N_2 adsorption system BET method. The density of GaHAp powders was determined by helium pycnometry. Ion release in Dulbecco's Modified Eagle Medium (DMEM) was measured for 18 days by Inductively Coupled Plasma Mass Spectrometry (ICP-MS). Biocompatibility of GaHAp was tested on human fibroblast BJ1 after 1, 3 and 7 days. For all the tests pure HAp was used as a control.

RESULTS: The obtained GaHAp showed characteristic peaks of apatite on XRD (Fig. 1). Additional gallium compound phases were not observed. Compared to pure HAp, decrease in crystallinity was observed. The obtained GaHAp has higher SSA than HAp (71±7 m^2/g), respectively 2wt% GaHAp: 95±5 m^2/g; 4wt% GaHAp: 117±4 m^2/g; 6.3wt% GaHAp: 109 ±2 m^2/g and 8wt% GaHAp: 102±5 m^2/g. Additionally, smaller particles were formed in case of GaHAp (d_{BET}). Ga^{3+} ions were constantly released through the 18 days with a release range of ~ 30 - 40%.

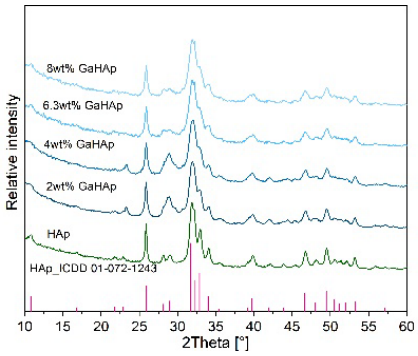

Fig. 1. XRD patterns of hydroxyapatite and gallium doped hydroxyapatite.

BJ1 fibroblasts exposed to GaHAp showed a cell viability of 90% after 7 days of culture compared to control. (Fig. 2).

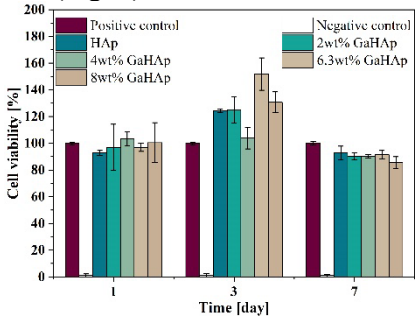

Fig. 2. Viability of BJ1 fibroblast after exposure to the different GaHAp paste compositions.

DISCUSSION & CONCLUSIONS: Presence of Ga^{3+} ions in the synthesis inhibits hydroxyapatite crystal formation resulting in a decrease in crystallinity and particle size. GaHAp allows a sustained release kinetic of Ga^{3+} ions. Also, none of GaHAp composite exhibited cytotoxic effect.

ACKNOWLEDGEMENTS: This research is funded by the EuroNanoMed III project "NANO delivery system for one-shot regenerative therapy of peri-implantitis" (ImlpantNano). Authors acknowledge financial support from the European Union's Horizon 2020 research and innovation programme under the grant agreement No 857287.

Formulation and Characterization of Novel Lipid Nanoparticles for the Delivery of Splice-Switching Oligonucleotide

M. Ojansivu[1], H.M.G. Barriga[1], M.N. Holme[1], S. Morf[1], T. Kjellman[2], M. M. Stevens[1,3]

[1]Department of Medical Biochemistry and Biophysics, Karolinska Institute, Stockholm, Sweden, [2]Camurus AB, Lund, Sweden, [3]Department of Materials, Department of Bioengineering and Institute of Biomedical Engineering, Imperial College London, UK

INTRODUCTION: Lipid nanoparticles (LNPs) have recently gained a lot of interest as safe and efficient drug delivery vehicles due to the success with COVID-19 vaccines and Onpattro® siRNA-LNP drug [1,2]. However, there are still large gaps in our knowledge of the LNP performance. Here, we aim to gain better understanding of the interplay between LNP composition, structure, and function.

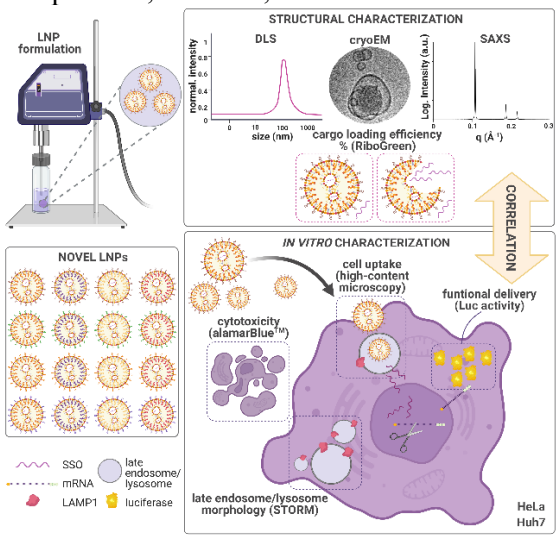

Fig. 1: Schematic illustration of the study workflow. Created with BioRender.

Table 1. Compositions of the novel LNPs.

C1/C2 base	Lipid 1/2	Stabilizer 1/2/3/4

METHODS: A schematic overview of this study is depicted in Fig. 1. LNPs were prepared by tip sonication and characterized with dynamic light scattering (DLS) and cryo electron microscopy (cryoEM). 16 different novel compositions (Table 1) were formulated. MC3 LNPs (Onpattro® composition) were used as a control. A splice-switching oligonucleotide (SSO), correcting a splicing error in a non-functional luciferase (Luc) gene in engineered HeLa and Huh7 cells [3], was used as LNP cargo and the cargo loading was determined with RiboGreen assays. Cytotoxicity of the LNPs was evaluated with alamarBlue™ assays, cell uptake with microscopy (Rhodamine B labelled LNPs) and functional delivery with Luc activity assays. The effect of LNPs on the late endosomes/lysosomes was assessed with stochastic optical reconstruction microscopy (STORM). Small-angle X-ray scattering (SAXS) was conducted to evaluate the phase structure of the lipid compositions.

RESULTS: LNPs were successfully formulated from all the novel compositions, and none of them showed cytotoxicity unlike the control MC3 LNPs (Onpattro® composition). LNPs with lipid 1 were better uptaken than LNPs with lipid 2. Functional SSO delivery was achieved only with lipid 1 LNPs with stabilizer 1 and C2 base composition. The Luc activity with these LNPs exceeded MC3 control in HeLa cells. LNPs increased lysosomal size even in the absence of functional delivery.

DISCUSSION & CONCLUSIONS: We identified a novel LNP composition which outperformed the gold standard LNPs (MC3) in HeLa cells. These LNPs had a more organized lattice structure compared to non-functional compositional counterparts, implying a link between structure and function. The novel and in-depth data collected in this project sheds lights on some of the key areas in the field on nanomedicine and LNP-mediated drug delivery.

ACKNOWLEDGEMENTS: M.O. was funded by the J. and A. Erkko, O.A. Malm, The Paulo and The O. Huttunen Foundations. This work was supported by the "FoRmulaEx" research centre (IRC15-0065). We thank Dr. M. Munson at Astra Zeneca for formulating the MC3 LNPs, Prof. Samir EL Andaloussi for donating the cell lines and N-O. Gustafsson, M. Johansson and J. Barauskas from Camurus for their input.

REFERENCES: [1] Suzuki and Ishihara, Drug Metab Pharmacokinet, **2021**, *v. 41*, 100424; [2] Akinc et al., Nat Nanotechnol., **2019**, *v. 14(12)*, p. 1084; [3] Rocha et al. Nucleic Acid Ther., **2016**, *v. 26(6)*, p. 381.

Antibacterial Properties of Additively Manufactured PVDF-Graphene Composites

A. Spanou[1,4], S. Panual[1], M. Taher[2,4], K. Welch[3], C. Persson[1]

[1]Department of Materials Science and Engineering, Biomedical Engineering, Uppsala University, Sweden, [2]Department of Chemistry - Ångström Laboratory, Uppsala University, Uppsala, Sweden, [3]Department of Materials Science and Engineering, Nanotechnology and functional materials, Uppsala University, Sweden, [4]Graphmatech AB, Uppsala, Sweden

INTRODUCTION: Antimicrobial resistance has become a leading cause of death around the world. An alternative to the use of antibiotics is inherently bacteriostatic or antibacterial material surfaces. Graphene has demonstrated such properties, but its effectiveness has not been fully explored as incorporated into polymers. Polyvinylidene fluoride (PVDF) is a biocompatible polymer already used in applications where antibacterial properties are important, such as sutures, surgical meshes and as sensors in implantable devices. [1]. Additive manufacturing could accommodate for the complex geometries often required for such applications. In this study the antibacterial properties of reduced graphene oxide (rGO) and graphene nanoplatelets (GnP), two forms of graphene suitable as polymeric additives, were examined in thermally compounded and additively manufactured PVDF samples.

METHODS: PVDF – graphene (6.5wt%) composite filaments were prepared in a twin screw compounder (PolyLab). The composites were subsequentially 3D printed using fused deposition modeling (Ultimaker S5+). Scanning electron microscopy (SEM) (Zeiss LEO 1530) was used to assess the arrangement of the graphene nanofillers in the polymer matrix.
The antibacterial properties were examined using surface contact tests. The viability of *Escherichia coli (E.coli)* and *Staphylococcus aureus (S. aureus)* was tested when exposed to the surface of the samples.

RESULTS: The GnP – PVDF composites showed a significant reduction of colony forming units for both *E.coli* and *S. aureus*, when compared with the PVDF reference. The rGO-PVDF composites on the other hand did not exhibit any significant difference to the PVDF reference. The difference in antibacterial effects could be derived from the morphology observed in the SEM images, where the samples with GnP showed sharp protrusions of the graphene flakes on the surface of the printed sample. Such morphology was not observed on the PVDF- rGO samples.

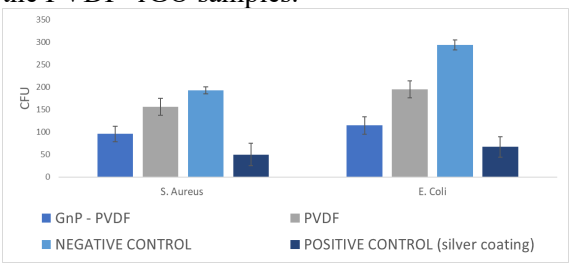

Fig. 1: Surface contact test results of PVDF-GnP composites for S. Aureus and E.Coli.

DISCUSSION & CONCLUSIONS: The antibacterial effect of GnPs is likely attributed to a physical mechanism involving physical distraction of the cell membrane due to the sharp edges of the species. Similar observations were made by Pandit *et al.* [2]. In previous studies on rGO, an antibacterial effect was observed where the mechanism of action was chemical, inducing oxidative stresses on the bacterial membrane [3]. Here, rGO was well integrated in the polymer matrix preventing it from chemically interacting with the bacteria. In conclusion, different graphene morphologies exhibit different antibacterial properties when incorporated into this polymeric matrix.

ACKNOWLEDGEMENTS: Support from Graphmatech AB and VINNOVA Competence Centre AM4Life (2019-00029) is gratefully acknowledged.

REFERENCES: [1] A.J.T. Teo et al., ACS Biomaterials Science & Engineering, **2016**, *v. 2*, p. 454; [2] S. Pandit et al., Advanced Materials Interfaces, **2018**, *v. 5*, 1701331; [3] S. Liu et al., ACS nano, **2011**, *v. 9*, p. 6971.

Microneedles Loaded with Vancomycin for Treatment of Skin Infections

J. Ziesmer[1], P. Tajpara[2], N.-J. Hempel[3], M. Ehrström[4], K. Melican[5], L. Eidsmo[2,6], G.A. Sotiriou[1]

[1]Department of Microbiology, Tumor and Cell Biology, Karolinska Institutet, Stockholm, Sweden; [2]Department of Medicine Solna, Karolinska Institutet, Stockholm, Sweden; [3]Department of Pharmacy, University of Copenhagen, Copenhagen, Denmark; [4]Department of Reconstructive Plastic Surgery, Karolinska University Hospital, Stockholm, Sweden; [5]Department of Neuroscience, Karolinska Institutet, Stockholm, Sweden; [6]Leo Foundation Skin Immunology Center, University of Copenhagen, Copenhagen, Denmark

INTRODUCTION: Intravenous administration of vancomycin (VAN) is one of the gold standards for treating skin infections caused by methicillin resistant *Staphylococcus aureus (*MRSA*)*. However, systemic administration of VAN possesses several disadvantages, such as side effects and an increased risk of antibiotic-resistance development against VAN. Meanwhile, the local concentrations of VAN in the skin remain low [1]. Microneedles (MN) can deliver a wide range of drugs locally to the skin. We propose the delivery of VAN via MN patches as a novel therapy route for the treatment of MRSA-associated skin infections.

METHODS: We produced VAN-loaded MN-patches with dissolvable needles and a non-dissolvable backing layer. To ensure sufficient mechanical stability to cross the skin barrier excised piglet and human skin was pierced and imaged. Furthermore, we assessed the drug permeation across and into the skin using Franz cell diffusion assays. Finally, we investigated the killing efficiency from our MN-patches against MRSA in vitro performing diffusion assays and ex vivo in MRSA-infected pork skin.

RESULTS: VAN-loaded MN patches showed successful penetration into the skin models. Tissue sections indicated successful skin penetration of sulforhodamine loaded MN patches. Franz cell diffusion assays revealed that after 10 min application of VAN-MN arrays around 25 µg/cm^2 of VAN permeates the skin within 24 h and around 55 µg/cm^2 is retained within the skin tissue afterwards.
Moreover, by performing an agar disk diffusion test we showed that the VAN released from MN patches had similar antibacterial activity against MRSA as antibiotic control disks. Finally, we successfully reduced bacterial growth of MRSA in an ex vivo porcine infection model after application of MN loaded with 100 µg VAN.

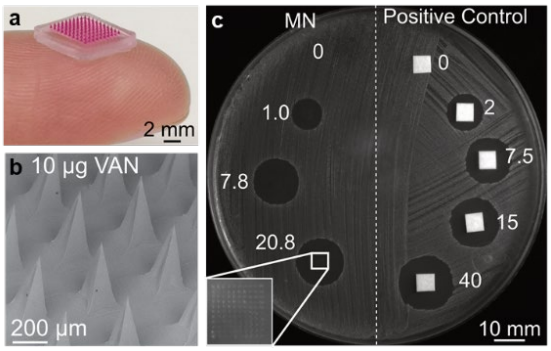

Fig. 1: a) Digital photograph of dye-loaded MN array. b) SEM image of MN array loaded with 10 µg VAN. c) Agar disk diffusion assay on MRSA after MN application loaded with different amounts of VAN, adapted from [2].

DISCUSSION & CONCLUSIONS: MN-patches are a potential new route for the administration of VAN against skin infection caused by MRSA.

ACKNOWLEDGEMENTS: This project has received funding from the European Research Council (ERC) under the European Union's Horizon 2020 research and innovation program (ERC Grant agreement N˚ 758705).

REFERENCES: [1] A. Savoldi et al., Curr. Opin. Infect. Dis., **2018**, *v. 31*, p. 120; [2] J Ziesmer et al., Adv. Mater. Technol., **2021**, *v. 6*, 2001307.

Sono-Responsive Hybrid Titanium Oxide/Polymer Nanomaterials Trigger Apoptosis in Cancer Cells Upon Ultrasound Irradiation

A. Sosnik[1], E. Peled[1], I. Zlotver[1]

[1]*Laboratory of Pharmaceutical Nanomaterials Science, Faculty of Materials Science and Engineering, Technion-Israel Institute of Technology, Haifa, Israel*

INTRODUCTION: Sonodynamic therapy (SDT) is a cost-effective, minimally invasive and localized anticancer therapy based on the *in situ* generation of reactive oxygen species (ROS) by combining low-intensity ultrasound (US), oxygen, and a sonosensitizer and it minimizes systemic toxicity. We investigated the sonodynamic performance of hybrid amorphous TiO_2/polymer nanomaterials and the pathway by which they kill cancer cells.

METHODS: Hybrid amorphous TiO_2/polymer nanoparticles were produced by a sol-gel process that comprises the synthesis and aging of a Ti(IV)-acetone oxo-organo complex, its mixing with different linear and branched poly(ethylene oxide)-poly(propylene oxide) (PEO-PPO) block copolymers and their nanoprecipitation in water [1].

RESULTS and DISCUSSION: Initially, we assessed the effect of PEO-PPO block copolymers of different architecture, molecular weight, and hydrophilic-lipophilic balance on the size, size distribution and morphology of the hybrid nanoparticles. Regardless of the PEO-PPO block copolymer used in the synthesis, the properties of the hybrid nanoparticles are governed by the age of the oxo-organo complex [2]. Morphological analysis by high resolution-transmission electron microscopy showed that all the nanoparticles are rounded. Next, we demonstrated that these hybrid nanoparticles induce the formation of ROS upon irradiation with therapeutic US. In addition, they exhibit good compatibility and uptake by the Rh30 cell line, a model of rhabdomyosarcoma (a pediatric tumor of connective tissue) and do not cause significant hemolysis upon exposure of up to 24 h. Finally, we investigated the pathway, by which these nanomaterials kill Rh30 cells using annexin-V/propidium iodide staining, and flow cytometry and demonstrate that, they trigger cell apoptosis (Fig. 1) [2].

CONCLUSIONS: To the best of our knowledge, this is the first work reporting on the sono-responsive performance of an amorphous TiO_2-based nanomaterial and its potential application in the SDT of cancer.

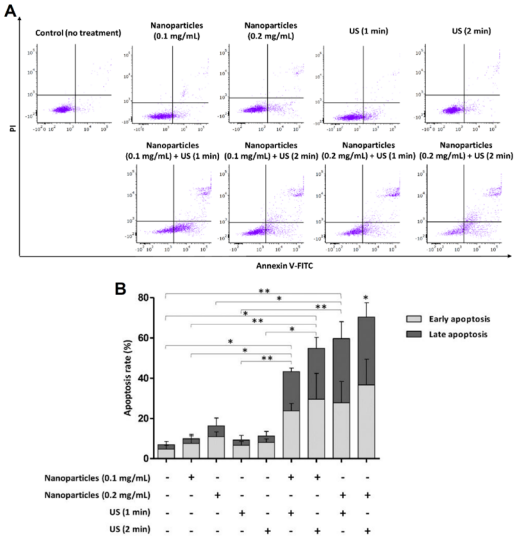

*Fig. 1. Apoptosic rate of Rh30 cells upon 24 h treatment without and with hybrid TiO_2/T1107-20 nanoparticles at an intensity of 1 W/cm^2 or control (untreated) cells, as determined by flow cytometry by using Annexin V-FITC/propidium iodide (PI) staining. (A) Representative dot plots of Rh30 cells treated without or with hybrid TiO_2/T1107-20 nanoparticles and without and with US irradiation. (B) Bar chart of apoptosis rate following incubation without or with hybrid TiO_2/T1107-20 nanoparticles and without and with US irradiation. Results were calculated as % of positive annexin V-FITC cells out of total cells counted. Data are presented as mean ± SD (n = 3). *Statistically significant difference between values by the t-test (p <0.05); **statistically significant difference between values by the t-test (p <0.01).*

ACKNOWLEDGEMENTS: This research was funded by the Israel Science Foundation (ISF Grant #327/19).

REFERENCES: [1] V. Kushnirov Melnitzer et al., Adv. Func. Mater., **2020**, *v. 30*, 1806146; [2] A. Pariente et al., Mater. Today Chem., **2021**, *v. 22*, 100613.

Spatial Transcriptomic Resolution of the Tissue-Material Interface in Wound Healing

A.T. Speidel[1], H. Autefage[1], A. Mollbrink[2], E. Müller[1], S.W. Park[1], C.S. Wood[1], Y.K.V. Chan[1], J. R. M. Ojala[1], M.M. Stevens[1,3]

[1]Division of Biomaterials, Department of Medical Biochemistry and Biophysics, Karolinska Institute, Stockholm, SE, [2]Science for Life Laboratory, Division of Gene Technology, KTH Royal Institute of Technology, Stockholm, SE, [3]Department of Materials, Department of Bioengineering, Institute of Biomedical Engineering, Imperial College London, UK

INTRODUCTION: The routine clinical translation of biomaterials is hampered by the poorly understood foreign body response (FBR). Through exploring the tissue-material interface of commonly used biomaterials in a wound healing model through high resolution methods like the Visium spatial transcriptomic technology, a deeper understanding of tissue-material interactions will allow for the design of smarter materials that may improve wound healing as well as lend insights into methods for ultimately circumventing the FBR.

METHODS: The storage (G'), loss (G"), and complex shear (G*) moduli of mouse skin and the material panel composed of alginate, collagen, poly(ethylene glycol) (PEG), and polyurethane-PEG (PU-PEG) hydrogels were assessed in oscillatory frequency and strain sweeps. Swelling and degradation profiles of the material hydrogel panel were assessed after fabrication (day 0) as well as after 1, 3, 7, and 14 days. Endotoxin content of the material panel components was confirmed to be well below the calculated 2.72 EU/mL through a chromogenic LAL assay. Animal work was conducted under ethical permit N240/15. Male 8 week old C57BL6J mice were anesthetized with 4% isoflurane. Hair was removed with hair removal cream and the skin was sterilized with 70% ethanol. Bilateral 5 mm wounds were created on the mouse backs and each wound received either alginate, collagen, PEG, PU-PEG hydrogel treatments held in place with a Tegaderm secondary material or controls with a Tegaderm only treatment or no treatment. The wound areas and mouse masses were monitored in studies over 2 and 14 days, at which point mice were sacrificed and their tissue was embedded fresh in OCT. Tissue sections were collected for assessment through histology or Visium analysis according to manufacturer's instructions. Visium data was processed with 10x Genomics' Space Ranger pipeline and underwent quality control, dimensionality reduction, cluster, and differential gene expression analysis in RStudio (2021.09.1, R version 4.1.2).

RESULTS: The compositions of the hydrogel materials were tuned to rheologically resemble mouse skin, exhibiting consistent average mechanical properties between 3-5 kPa across physiologically relevant frequencies. Synthetic covalently crosslinked materials, PEG and PU-PEG exhibited swelling capacities roughly 2x and 5x lower than natural-derived ionically crosslinked alginate and physically crosslinked collagen materials, respectively. Of the materials in the panel only alginate displayed significant degradation after 14 days *in vitro*. Wound closure profiles of the material panel-treated wounds were all similar across the 14-day study. Untreated wounds showed more rapid closure and Tegaderm-treated control wounds showed delayed closure compared with the material panel-treated wounds through the first 3 days of the wound healing study. Visium analysis enables spatial resolution of the full gene expression profiles across the tissue-material interface and extent that the wound environment extends into the surrounding skin tissue. Cluster analysis successfully identifies known layers of skin and distinguishes the material panel treated wounds from the untreated and healthy skin controls.

DISCUSSION & CONCLUSIONS: Material treatment of the wound environment alters the early wound closure rate and the gene expression profile of wound tissue profile at the material-tissue interface.

ACKNOWLEDGEMENTS: The data handling in project SNIC 2021/22-972, 23-702 provided by SNIC at UPPMAX, partially funded by SRC 2018-05973. Funding provided through VR 2015-02904, Stiftelsen Lars Hiertas Minne FO2017-0210, Wenner-Gren Siftelserna UPD2017-0254, 2018-0269, StratNeuro 2018, KI research foundation 2018-01643.

Micropathological Bone Chip Modelling the Neurovascular Unit for Drug Delivery Systems Testing

E. Neto[1,2], A.C. Monteiro[1,2], C.L. Pereira[1,2], B. Sarmento[1,2,3], M. Lamghari[1,2]

[1]INEB - Instituto Nacional de Engenharia Biomédica, Universidade do Porto, Porto, Portugal, [2]i3S – Instituto de Investigação e Inovação em Saúde, Universidade do Porto, Porto, Portugal, [3]CESPU, Instituto de Investigação e Formação Avançada em Ciências e Tecnologias da Saúde, Gandra, Portugal

INTRODUCTION: Organ-on-a-chip *in vitro* platforms offer the ability to recapitulate and dissect mechanisms of physiological and pathological settings, as well as an accurate tool for drug screening and development of new therapeutic targets. Bone diseases, such as osteoarthritis, comprise the action of inflammatory mediators leading to a de-regulation of sensory innervation and angiogenesis. Although there are models to mimic bone vascularization or innervation, *in vitro* platforms merging the complexity of bone, vasculature, innervation and inflammation are missing.

In this study, we propose a microfluidic-based NeuroVascularized Bone chip (NVB chip) to 1) model the mechanistic interactions between innervation and angiogenesis in the inflammatory bone niche, and 2) explore as a screening tool of novel strategies targeting inflammatory diseases, using a nano-based drug delivery system.

METHODS: We set a novel microfluidic-based design to incorporate different cells in culture concerning their *in vivo* interaction. The design comprised three different compartments to accommodate neuronal (sensory neurons), endothelial (human umbilical vein endothelial cells (HUVEC)) and bone cells (osteoclasts). Ibuprofen-loaded nanoparticles were tested in bone compartment under inflammatory Il-1b stimuli.

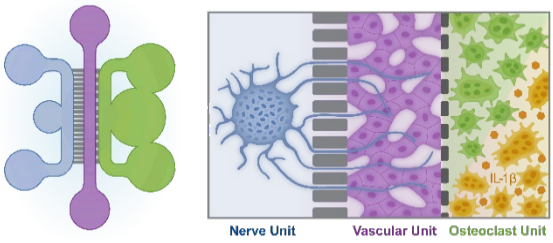

Fig. 1. Model for NeuroVascular Bone chip (NVBchip).

RESULTS: We were able to set the optimized conditions (cell density and time of culture) for the different cell types, starting with endothelial cells, then osteoclasts and finally sensory neurons. We showed the formation of lumen-like structures inside the chip and a reduction in the permeability along the culture time.

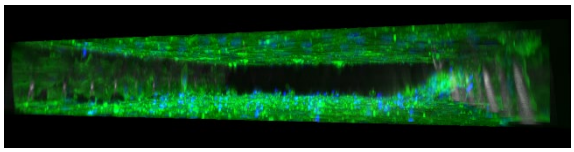

Fig. 2. Lumen-like structure at day 1 in microfluidic.

Osteoclasts were cultured under non-inflammatory and inflammatory conditions and characterization of pro-inflammatory and angiogenic profiles was performed. Neuronal cells were then added to the system and axonal growth was quantified. Under inflammatory conditions, it was observed a higher axonal growth and a decrease in the endothelial barrier permeability. The axonal growth was reverted in the presence of ibuprofen-loaded nanoparticles.

CONCLUSIONS: We consider that we have transposed into a single chip the key cellular players and the cascade of events that are likely to occur in bone inflammatory pathologies. This neurovascular bone model will be a useful platform to carry out studies such as validation and comparative therapeutic tests with the opportunity to perform the administration in the vascular compartment and assess the drug effects axonal and bone cells functions.

ACKNOWLEDGEMENTS: This work has received funding from the European Union's Horizon 2020 research and innovation programme under grant agreement No 953121 (FLAMIN-GO – From pathobiology to synovia on chip: driving rheumatoid arthritis to the precision medicine goal).

Combination of Live Cell Imaging and QCM-D to Study Cell-implant Interactions

D.S. Zaytseva-Zotova[1], A. Barrantes[1], H. Tiainen[1]

[1]*Department of Biomaterials, Institute of Clinical Dentistry, University of Oslo, Oslo, Norway*

INTRODUCTION: Medical implants play an increasingly important role in clinical practice. Unfortunately, the implant failure rate remains high. One of the determinants of the implant failure is its insufficient tissue integration and lack of interaction with the cells from the surrounding tissues. Quartz Crystal Microbalance with Dissipation (QCM-D) is a highly sensitive real-time label-free technique that can be used to study mechanisms at the interface between cells and implants (< 250 nm) [1]. QCM-D instrument senses small mass changes on the surface of a quartz crystal covered with a biomaterial of interest and allows to measure changes in thickness and viscoelastic properties of the adsorbed layer. In this work we aimed at combining the QCM-D sensing approach with live cell imaging to study fibroblast adhesion on titanium surfaces under different experimental growth conditions.

METHODS: Cell attachment to Ti was monitored in a QCM-D QSense® window module (QWM 401) using a QCM-D QSense® E4 (QSX 310, Biolin Scientific) and Leica SP8 upright confocal laser scanning microscope (CLSM) with 10×/0.4 dry objective. Ti sensors (QSX 310) were prepared according to the manufacturer's protocol, equilibrated at 37ºC in serum-free medium for 1 hour and after that in a respective test medium at 50 µl/min for approximately 1 hour. Primary human gingival fibroblasts were stained with 1 µM CellTracker™ Green CMFDA dye (Invitrogen) for 30 min at 37ºC and then injected into a QCM module at 300 µl/min (30 sec) at a concentration of 0.5 × 10^6 cells/ml. Measurements were performed at 37ºC under flow (10 µl/min) of test medium supplemented with 0.1 µM propidium iodide to visualise dead cells [2]. Time-lapse images were taken with 15 min intervals (CLSM) and changes in frequency and dissipation (ΔD) were monitored continuously (QCM-D) during 16 hours. Changes in cell number, viability, morphology (area) and motility were analysed in ImageJ.

RESULTS: Cell adhesion kinetics, morphology and motility were different in media supplemented with 0, 1 and 10% FBS. Fibroblasts readily attached and spread on the Ti surface in medium without FBS but showed low motility and activity (Fig.1). In contrast, cell adhesion kinetics was slower and cell motility was higher in presence of FBS. Surprisingly, cells travelled longer distances in 1% FBS than in 10% FBS. The QCM-D showed that shifts in dissipation (ΔD) increased in the following order: 1 < 10 < 0% FBS (Fig. 1, right).

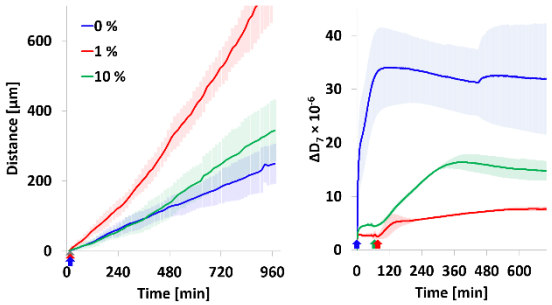

Fig. 1: Effect of serum concentration on accumulated distance travelled by gingival fibroblasts (left) and dissipation shifts (overtone 7, right). Blue, red and green represent 0, 1 and 10% FBS, respectively. Arrows show time of cell injection.

DISCUSSION & CONCLUSIONS: Our results show that cell motility and changes in dissipation are positively correlated. This points to the fact that ΔD-response can be used as a useful indicator for an indirect estimation of the number of focal adhesions [3].

ACKNOWLEDGEMENTS: This work has been supported by The Research Council of Norway (# 302590).

REFERENCES: [1] C. Fredriksson et al., J. Mater. Sci.: Mater. Med., **1998**, *v. 9*, p. 785; [2] C. Krämer et al., Sci. Rep., **2016**, *v. 6*, 32104; [3] A.M. Esfahani et al., Anal. Chem., **2018**, *v. 90(17)*, p. 10340.

Comparative Analysis of Corrosion Resistance Between CP-Ti, Ti-6Al-4V, and Novel Ti-Nb-Zr-Si Alloy in Phosphate Buffered Saline Solution

A. Bordbar-Khiabani[1], M. Gasik[1]

[1]*School of Chemical Engineering, Aalto University Foundation, Espoo, Finland*

INTRODUCTION: Titanium alloys have been widely used as biomaterials. The ternary Ti-Nb-Zr alloys were reported to exhibit a better corrosion resistance and biocompatibility in comparison with CP-Ti and Ti-6Al-4V due to the formation of compact and thicker passive film [1]. Recent studies demonstrate that Si plays an important role in modifying the elastic modulus and mechanical strength of Ti-based alloys [2], and possesses very good osseointegration properties [3], so it can be used as a good alloying element to develop the Ti-Nb-Zr-Si (TNZS) alloy for medical implant applications. In this work, the electrochemical corrosion resistance of the TNZS alloy were compared to those of the CP-Ti and Ti-6Al-4V in phosphate buffered saline (PBS) solution.

METHODS: The disc-type CP-Ti, Ti-6Al-4V, and TNZS samples with a diameter of 15 mm were polished with SiC grit 1200 paper. The electrochemical tests were performed in 37 °C PBS solution with air + 5% CO_2 gas bubbling using IviumStat in a three-electrode system with a graphite rod as the counter electrode and Ag/AgCl as reference electrode. Before tests, samples with area of 1 cm^2 were immersed in the PBS solution for 1 h to allow the open circuit potential (OCP) stabilize. The potentiodynamic polarization (PDP) curves were scanned at a rate of 1 $mV.s^{-1}$. The electrochemical impedance spectroscopy (EIS) tests were conducted at an OCP by applying a 10 mV sinusoidal potential through a frequency domain from 100 kHz down to 100 mHz. The EIS plots were analyzed using ZView software.

RESULTS: The PDP curves of samples are shown in Fig. 1a. The corrosion potential (E_{corr}) of TNZS was more positive with the value of -0.11 V in comparison to Ti-6Al-4V (-0.56 V), and CP-Ti (-0.74 V). The corrosion current density (i_{corr}) of TNZS (4.67 $\mu A.cm^{-2}$) was decreased compared to that of Ti-6Al-4V (6.81 $\mu A.cm^{-2}$), and was also lower than CP-Ti (9.32 $\mu A.cm^{-2}$). Fig. 1b and c show the EIS plots. The equivalent circuit (Fig. 1d) consists of the two time constants: one is attributed to the charge transfer resistance (R_{ct})/double layer capacitance (C_{dl}) parallel combination, and the second is attributed to the film resistance (R_{film})/film capacitance (C_{film}) parallel combination. The R_{film} values were obtained 33.5, 19.8, and 9.6 $k\Omega.cm^2$ for TNZS, Ti-6Al-4V, and CP-Ti, respectively.

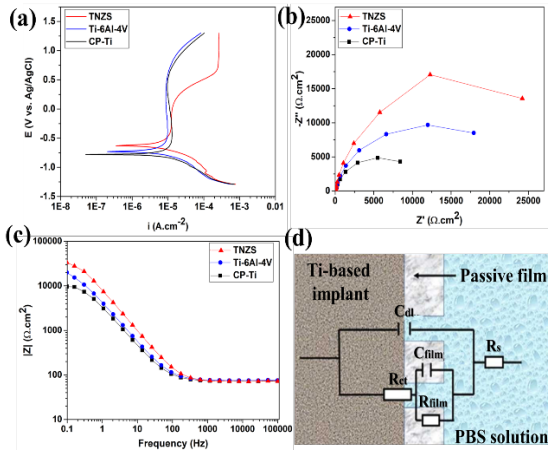

Fig. 1: (a) PDP curves, (b) Nyquist plots, (c) Bode plots, and (d) equivalent circuit.

DISCUSSION & CONCLUSIONS: The TNZS alloy had lower i_{corr} and higher E_{corr} values than the Ti-6Al-4V and CP-Ti, showing the lower corrosion rate of TNZS. It has been reported that Ti-13Nb-13Zr alloy possesses a high corrosion potential of -2.32 V due to the thicker and defect-less passive layer, resulting in addition of Nb and Zr to Ti [1]. As seen in Fig. 1b and c, the radius of a semi-circular arc for TNZS and Bode modulus value are higher than others, indicating the passive oxide film of TNZS has better polarization resistance. In conclusion, the results indicate that the TNZS alloy exhibits high corrosion resistance in PBS.

ACKNOWLEDGEMENTS: This study has received funding from the MSCA ITN under grant agreement no. 860462 for "PREMUROSA" project.

REFERENCES: [1] P.F. Ji et al., Corr. Sci., **2020**, *v. 170*, 108696; [2] A.M.G. Tavares et al., J. Mech. Behav. Biomed. Mater., **2015**, *v. 51*, p. 74; [3] L.Wang et al., Mater. Lett., **2014**, *v. 116*, p. 35.

Oxidised Silicon Nitride for the Inactivation of SARS-CoV-2

I. Katsaros[1], J. Ling[2], G.Akusjärvi[2], Å. Lundkvist[2], C. Persson[3], W. Xia[1], H. Engqvist[1]

[1]Division of Applied Materials Science, Department of Materials Science and Engineering, Uppsala University, Uppsala, Sweden, [2]Department of Medical Biochemistry and Microbiology, Uppsala University, Uppsala, Sweden, [3]Division of Biomedical Engineering, Department of Materials Science and Engineering, Uppsala University, Uppsala, Sweden

INTRODUCTION: The global COVID19 pandemic caused by the severe acute respiratory coronavirus (SARS-CoV-2) has emphasized the need for measures to limit the spread of dangerous pathogens. Utilising antiviral materials along with the establishment of personal protection measures can further hinder viral spread. Silicon nitride (Si_3N_4) is a material that has been shown[1] to be effective at inactivating pathogens through the micro-elution of biocidal ammonia from its surface. Properties like surface charge and hydrophilicity of Si_3N_4 can be manipulated through surface modifications to maximise pathogen attachment and inactivation. In this study we present a surface modified silicon nitride material aimed at increased absorption and inactivation of SARS-CoV-2.

METHODS: Silicon nitride powders were heat treated at 1070° C for 7h as a way to increase the material's hydrophilicity and negative charge as both these surface properties have been shown to improve SARS-CoV-2 attachment[2]. The effects of the heat treatment on the material were examined through transmission electron microscopy, X-ray photoelectron spectroscopy, X-ray diffraction and water contact angle measurements. SARS-CoV-2 viral solutions were brought in contact with test materials and controls for one, ten and 60 minutes. Thereafter, viral infectivity and viral RNA fragmentation were examined through plaque forming unit and real time quantitative polymerase chain reaction assays, respectively. For the plaque forming unit assay, epithelial Vero E6 cells were utilised. Copper and untreated viral solutions were used as positive and negative controls, respectively.

RESULTS: The heat treatment resulted in an approximately twice as hydrophilic material. The surface of the material was comprised mainly of silicon dioxide with low amounts of nitrogen, the driving force behind the antiviral properties of the material. Nevertheless, the material was highly effective at reducing viral infectivity at both room and homeostatic temperatures. Furthermore, the genome of viruses brought in contact with Si_3N_4 was fragmented at a higher rate compared to copper.

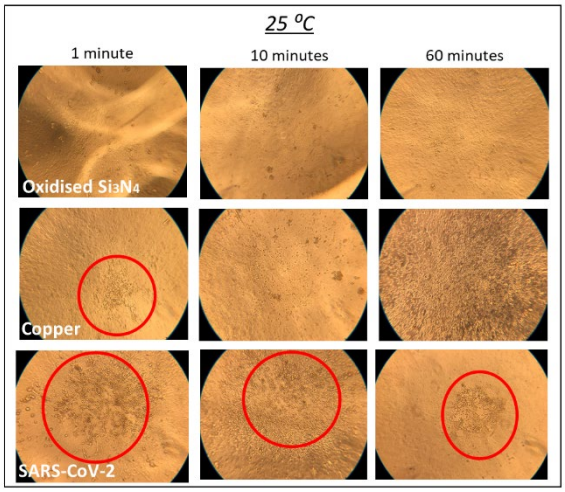

Fig. 1 The cytopathic effect that came as a result of viral infection of Vero E6 cells is noted by red circles. Samples infected with the virus brought in contact with the oxidized silicon nitride showcased a normal morphology and no signs of infection.

DISCUSSION & CONCLUSIONS:
This study clearly showed that the oxidised silicon nitride material was highly effective at inactivating SARS-CoV-2 as quickly as after one minute of contact. The results of this study indicate that the material that was specifically engineered for antiviral applications could be used as a tool in the fight against viral spread.

ACKNOWLEDGEMENTS: This project has received funding from the European Union's Horizon 2020 research and innovation programme under the Marie Sklodowska-Curie grant agreement No 812765.

REFERENCES: [1] G. Pezzotti et al., Sci. Rep., **2021**, *v. 11(1)*, p. 2977; [2] E. Joonaki et al., Chem., **2020**, *v. 6(9)*, p. 2135.

Electrophoretic Deposition of Multi-layered Antibacterial and Bioactive Coatings on Chemically Pre-treated Titanium for Biomedical Applications

Z. Hadzhieva[1], A.R. Boccaccini[1]

[1]*Institute of Biomaterials, Department of Materials Science and Engineering, University of Erlangen-Nuremberg, Erlangen, Germany*

INTRODUCTION: The long-term stability of metallic implants presents a major challenge in orthopaedic applications due to their poor osseointegration and susceptibility to bacterial infections [1]. Coatings which are able to promote the bone-binding ability of the device while releasing antibacterial agents in a controlled manner in-situ, can be used to enhance the biological performance of the metallic implant. Among different coating techniques, electrophoretic deposition (EPD) benefits from simple processing equipment, versatility to coat complex shapes and the possibility to control the properties of the deposit by varying the process parameters [2]. Thus, the current work aims to develop novel composite polymer-based coatings with tailored bioactivity and antibacterial activity on titanium by EPD.

METHODS: Bioactive and antibacterial double-layered composite coatings composed of biopolymers, copper-doped bioactive glass particles (CuBG) and herbal drugs were prepared on chemically pre-treated titanium substrates by EPD. A top layer of chondroitin sulphate (CS) and CuBG was deposited on zein coating loaded with berberine chloride (BBR) on untreated, HCl-, NaOH- or H2O2-etched titanium. Statistical tools were used to optimize the deposition parameters of both layers, while the deposition mechanisms were explained by zeta potential measurements of the EPD suspensions. Moreover, the morphology, chemical composition, wettability, drug release behaviour, bioactivity, adhesion strength to the substrate and antibacterial properties of the coatings were analysed.

RESULTS: Scanning electron microscopy (SEM) demonstrated that the CuBG particles were homogeneously embedded in the polymeric matrix, while the presence of all coating components was confirmed by Fourier-transform infrared spectroscopy (FTIR). The double layer coatings on NaOH-treated titanium showed a critical load of 17±1 N, which is almost four times higher than the scratch resistance of the deposits on untreated substrates. In addition, the chemical pre-treatment of titanium decreased the water contact angle of the composite coatings. Coatings deposited on NaOH-treated titanium exhibited enhanced bioactivity as apatite formation could be detected after 3 days of immersion in simulated body fluid (SBF), according to FTIR, SEM and EDX analyses. The double-layered coatings showed sustained release of berberine chloride and lower reduction of AlamarBlue in the presence of the Gram-negative bacterial strain *E. coli*.

DISCUSSION & CONCLUSIONS: The results of the current work suggest that the chemical pre-treatment of the titanium substrates prior to EPD significantly improved the scratch resistance and hydrophilicity of the double-layered CS-CuBG/zein-BBR coatings. Additionally, the deposition of a CS-CuBG top layer on the zein-BBR bottom layer delayed the drug release without affecting the bioactivity of the coatings. Finally, the coatings showed antibacterial efficacy against Gram-negative *E. coli*. In conclusion, double-layered composite coatings containing CS, CuBG, zein and BBR can be promising candidates to facilitate bone tissue integration and to prevent infections around orthopaedic implants.

REFERENCES: [1] K. Prasad et al., Materials, **2017**, *v. 10*, p. 884. [2] E. Avcu et al., Progress in Materials Science, **2019**, *v. 103*, p. 69.

Multifunctional Nanostructured Implant Coatings with Antibacterial Properties and Osseointegration Potential

F.J. Geissel[1], G.A. Sotiriou[1]

[1]*Department of Microbiology, Tumor and Cell Biology, Karolinska Institutet, Stockholm, SE*

INTRODUCTION: The increasing antimicrobial resistance (AMR) to antibiotics and the ability of most microbes to form a biofilm cause many revision surgeries of infected implants. The successful implant does not only exert antibacterial properties, but also promotes the integration with the host tissue (osseointegration). For this reason, a multifunctional coating consisting of bioglass (BG), and silver (Ag) nanoparticles (NPs) is investigated.

METHODS: Flame spray pyrolysis (FSP) is used to synthesize a multicomponent coating consisting of Ag and BG NPs and to deposit it on medical grade titanium substrates in a single step. Four different mass fractions of Ag (stated as xAgBG) are prepared: x = 0, 10, 20 and 50 wt%. X - ray diffraction (XRD), scanning electron microscope (SEM) and transmission electron microscope (TEM) characterize the composition / morphology. The Ag^+ - release is measured electrochemically and is studied for the four different mass fractions of Ag. *S. aureus* biofilm growth inhibition for 0AgBG is compared to the different Ag loadings. The bioactivity of the samples is evaluated by incubating them in simulated body fluid (SBF). After different time points the samples are gently washed, dried and analysed with Fourier-transform infrared spectroscopy (FTIR) and SEM. A texture analyser with a custom made facete evaluated the critical adhesion force and compared it between samples before and after flame annealing. Finally, the biocompatibility and osteogenic potential of the samples were tested with Alamar blue, collagen activity and ALP assays.

RESULTS: TEM images of the corresponding powders show the Ag NPs on the BG matrix with a larger size for increasing Ag-content (Figure 1). The coatings show a very homogeneous and porous surface. The 50AgBG samples inhibits *S. aureus* biofilm growth by almost 3 logs while the 20AgBG coating reduces it by 1 log (statistically significant). Both 0 and 20AgBG show hydroxyapatite formation after 24 hours, however only the pure BG (0) forms a thick layer.

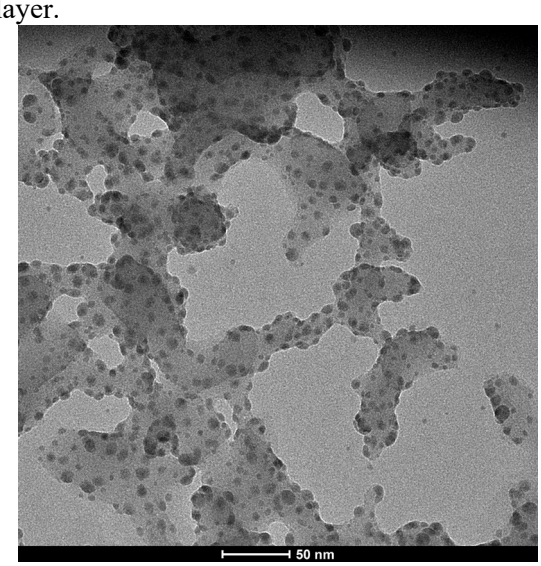

Fig. 1: TEM image of the 20AgBG NPs.

DISCUSSION & CONCLUSIONS: Homogenous multifunctional implant coatings consisting of Ag and BG NPs were successfully synthesised in a single step using FSP. The high surface area originating from small particle sizes shows a high antibacterial response. The samples are also bioactive, due to the formation of a hydroxyapatite layer after soaking in SBF. In-situ flame annealing increased the stability of the coatings which is crucial for potential applications. Here we present a stable implant coating for both antibacterial properties and osseointegration which could help to increase the success rate of implants and reduce expensive revision surgeries in the future.

ACKNOWLEDGEMENTS:
This project has received funding from the European Research Council (ERC) under the European Union's Horizon 2020 research and innovation programme (ERC Grant agreement n° 758705). Funding from the Karolinska Institutet Board of Research, the Swedish Research Council (2016-03471), the Jeansson Foundations (JS2016-0029) and the Åke Wiberg Foundation (M16-0098) is kindly acknowledged.

Comparing the Metal-electrolyte Interface During *In Vitro* Degradation of Mg-, Zn- and Fe-alloys

C. Wang[1], M.L. Zheludkevich[1,2], S.V. Lamaka[1]

[1]*Institute of Surface Science, Helmholtz-Zentrum Hereon, Geesthacht, Germany,* [2] *Institute for Materials Science, Faculty of Engineering, Kiel University, Germany*

INTRODUCTION: The biodegradable metals, such as Mg-, Zn- and Fe-alloys, have attracted research interest owing to their unique ability to dissolve after fulfilling the purpose of temporary implant (*e.g.* stent, screw or plate). The degradation process involves oxidation and reduction reactions which result in local acidification and alkalinisation of interface electrolyte. Established local acid-base equilibria are linked with the events of localized corrosion and formation of specific corrosion products. In this work, we summarise our recent studies [1-4] and compare the evolution of local pH, concentration of dissolved gaseous hydrogen and oxygen in HBSS electrolyte at the interface for three types of metallic samples: Mg-, Zn- and Fe-alloys.

METHODS: The setup custom developed for *in vitro* measurements is based on a commercial SVET-SIET equipment by Applicable Electronics with additionally integrated thermostat, peristaltic pump and CO_2 controller activated through a solenoid valve. The microelectrodes (tip diameter 2-50 micron) were integrated in the flow-through electrochemical cell by using LV4 software and the software of their suppliers: Unisense for potentiometric pH and amperometric H_2 micro-electrodes and Pyroscience for O_2 sensitive micro-optodes. Using motorized micro-manipulators, the microprobes were positioned 10-100 micron above the surface of the metallic samples degrading in HBSS (Hank's balanced salt solution). The evolution of local pH, concentration of dissolved H_2 and O_2 were recorded upon the first contact of the metal sample with the electrolyte and then during 24 hours.

RESULTS, DISCUSSION & CONCLUSIONS: Local electrochemical measurements revealed a number of unexpected features for each of the examined metallic samples. These include: only mild alkalinization 7.5-8.0 (rather than commonly expected pH above 10) and oxygen consumption, as secondary cathodic process during degradation of Mg-alloys; slight local acidification, causing pitting corrosion, during degradation of Zn- and Fe-alloys; hydrogen evolution (along with major oxygen reduction) during degradation of Zn. The common finding for all the metals is a major contribution of Ca^{2+} (when present together with carbonate and phosphate) to formation of precipitates that slow down the degradation of all the alloys and stabilizes pH at values close to neutral due to formation of hydroxyapatite species.

ACKNOWLEDGEMENTS: Mr. Cheng Wang thanks China Scholarship Council funding No.201806310128.

REFERENCES: [1] C. Wang, C. Tonna, D. Mei, J. Buhagiar, M.L. Zheludkevich, S.V. Lamaka, Biactive Materials, **2022**, *v. 7.*, p. 412; [2] C. Wang, X. Liu, D. Mei, M. Deng, Y. Zheng, M.L. Zheludkevich, S.V. Lamaka, Corros. Sci., **2022**, *v. 197*, 110061; [3] C. Wang, C. Song, D. Mei, L. Wang, W. Wang, T. Wu, D. Snihirova, M.L. Zheludkevich, S.V. Lamaka, Corros. Sci., **2022**, *v. 197*, 110059; [4] C. Wang, D. Mei, G. Wiese, L.Q. Wang, M. Deng, S.V. Lamaka, M.L. Zheludkevich, npj Mater. Degrad., **2020**, *v. 4*, art. nr. 42.

Novel Bioactive Materials for Biomedical Implants

J.V. Rau[1]

[1]*Istituto di Struttura della Materia, Consiglio Nazionale delle Ricerche (ISM-CNR), Via del Fosso del Cavaliere 100, 00133 Rome, Italy*

INTRODUCTION: Due to the trend in demographics towards older population, there is currently a dramatic increase in the use of implants to substitute various parts of the human body. The present multidisciplinary research regards the new trends in biomaterials' design to satisfy the requirements posed by modern medicine to biomedical implants, such as the orthopaedic and dental ones. The efforts are mainly directed to improve the implants' long term stability and osseointegration, as well as to develop new biodegradable implant materials possessing antimicrobial properties. Regarding the long term stability, an important issue is a high risk of infections caused by bacteria attached to the implant surface and their resistivity to the commonly used antibiotics. Among the other important challenges to be considered are the host tissue healing and regeneration, triggered by materials. In this work, the coating materials for titanium and Mg- and Zn-based biodegradable implants were developed. Coatings based on substituted biomimetic calcium phosphates [1] and bioactive glasses were investigated.

METHODS: For bulk material synthesis, the Sol-Gel method was used. For coating deposition, the Pulsed Laser Deposition technique and the Radiofrequency Magnetron Sputtering method were applied. For materials characterization, Scanning and Tunnelling Electron Microscopies; Atomic Force microscopy; X-ray diffraction; FTIR, Raman and X-ray photoelectron spectroscopies; micro and nano-indentation techniques were used. *In vitro* bioactivity tests in Simulated Body Fluid, microbiology and cell tests were performed.

RESULTS: The recent results obtained for several novel compositions of ion doped calcium phosphate and bioactive glass-ceramic coatings regard materials releasing Zn^{2+}, Cu^{2+}, and Sr^{2+} ions from substituted hydroxyapatites; Ag^{+} and Fe^{3+} ions from substituted tricalcium phosphates; and Mn^{2+} ions from bioactive glasses. In this work, we used the glancing angle deposition (GLAD) approach as a promising tool to achieve high ratio coating surface nanopatterning and gradient structures to influence bacteria and stem cell fate [2]. The deposited coatings are characterized by inclined columnar-like structures with variations at the nano-roughness level and a direction of growth allowing to obtain patterned structures with different shapes and sizes (see Fig. 1). This type of coatings has attracted attention due to the possibility of controlling the level of porosity and roughness, and due to their peculiar mechanical characteristics.

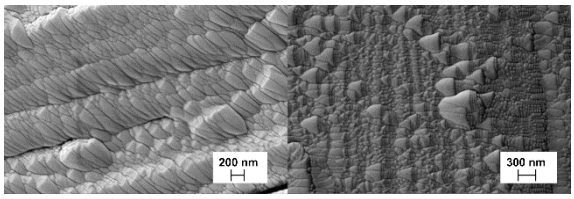

Fig. 1: The difference in coatings' morphology between Cu^{2+} substituted calcium phosphate (left) and Zn^{2+} substituted calcium phosphate (right) deposited using GLAD under equal working conditions.

The obtained results suggest for a synergetic effect of antibacterial activity due to the Zn^{2+} and Cu^{2+} ions presence and a decrease in the bacterial attachment due to the high aspect ratio nanopatterning.

DISCUSSION & CONCLUSIONS: Present research, performed in collaboration with several research groups, suggests that novel hierarchical micro- and nanostructured materials can be particularly relevant for new strategies in tissue replacement and regeneration, ensuring suitable structural, chemical, morphological and mechanical characteristics, improving osseointegration of dental and orthopaedic medical implants and providing a controlled release of active principles, in particular, against infections.

REFERENCES: [1] K.A. Prosolov et al. Coatings, **2019**, *v. 9*, p. 220; [2] I.V. Fadeeva et al. Materials, **2020**, *v. 13(19)*, p. 4411.